

AD 729212

ETR-TR-71-4

VARIATIONS IN ORBITAL ELEMENTS

James A. Ward, Jr., RCA International Service Corporation

August 1971



DDC
RECEIVED
SEP 9 1971
B ."

Reproduced by
NATIONAL TECHNICAL
INFORMATION SERVICE
Springfield, Va. 22151

APPROVED FOR PUBLIC
RELEASE; DISTRIBUTION
UNLIMITED

Instrumentation and Data Processing Division
Directorate of Range Operations
Air Force Eastern Test Range (AFSC)
Patrick Air Force Base, Florida

87

Unclassified

Security Classification

DOCUMENT CONTROL DATA - R&D		
(Security classification of title, body of abstract and indexing annotation must be entered when the overall report is classified)		
1. ORIGINATING ACTIVITY (Corporate author) RCA International Service Corporation Missile Test Project Patrick Air Force Base, Florida		2a. REPORT SECURITY CLASSIFICATION Unclassified - does not contain restricted data. 2b. GROUP N/A
3. REPORT TITLE Variations in Orbital Elements		
4. DESCRIPTIVE NOTES (Type of report and inclusive dates)		
5. AUTHOR(S) (Last name, first name, initial) Ward, James A., Jr.		
6. REPORT DATE August 1971	7a. TOTAL NO. OF PAGES 81	7b. NO. OF REFS 10
8a. CONTRACT OR GRANT NO. RCA Subcontract #71-0040-01 PAA Contract F08606-68-C-0040	8a. ORIGINATOR'S REPORT NUMBER(S) None	
c. d.	8b. OTHER REPORT NO(S) (Any other numbers that may be assigned this report) ETR-TR-71-4	
10. AVAILABILITY/LIMITATION NOTICES Approved for public release; distribution unlimited		
11. SUPPLEMENTARY NOTES None	12. SPONSORING MILITARY ACTIVITY Instrumentation Systems Analysis Branch Instru. and Data Processing Div., AFETR	
13. ABSTRACT Due to perturbative forces acting on a near earth satellite, the associated classical Keplerian orbital elements vary with time. These variations are divided into secular, short period and long period. The mathematical equations expressing these variations are presented without derivation along with numerical examples. A discussion of the practical applications of these variations to trajectory generation and orbit determination is included.		

DD FORM 1473
1 JAN 64

Unclassified

Security Classification

NOTICES

Qualified users may obtain copies of this report from the Defence Documentation Center.

When U. S. Government drawings, specification, or other data are used for any purpose other than a definitely related Government procurement operation, the Government thereby incurs no responsibility nor any obligation whatsoever, and the fact that the Government may have formulated, furnished or in any way supplied the said drawing, specification or other data, is not to be regarded by implication or otherwise, or in any manner licensing the holder or any other person or corporation, or conveying any rights or permission to manufacture, use or sell any patented invention that may in any way be related thereto.

Do not return this copy. Retain or destroy.

RECESSION FOR	
DCSTI	WHITE SECTION <input checked="" type="checkbox"/>
DDC	DIFF. SECTION <input type="checkbox"/>
UNANNOUNCED	<input type="checkbox"/>
JUSTIFICATION	
BY	
DISTRIBUTION/AVAILABILITY CODE	
DATE	AVAIL. NO. OF COPIES
A	

**BLANK PAGES
IN THIS
DOCUMENT
WERE NOT
FILMED**

14	KEY WORDS	LINK A		LINK B		LINK C	
		ROLE	WT	ROLE	WT	ROLE	WT
	Orbital Elements Secular variations Short period variations Long period variations Trajectory generation Orbit determination						

ABSTRACT

Due to perturbative forces acting on a near earth satellite, the associated classical Keplerian orbital elements vary with time. These variations are divided into secular, short period and long period. The mathematical equations expressing these variations are presented without derivation along with numerical examples. A discussion of the practical applications of these variations to trajectory generation and orbit determination is included.

VARIATIONS IN ORBITAL ELEMENTS

James A. Ward, Jr.
RCA Missile Test Project

APPROVED FOR PUBLIC
RELEASE; DISTRIBUTION
UNLIMITED

FOREWORD

This unclassified technical report was prepared under sub-contract No. 71-0040-01 by In-Flight Analysis & Programming, Data Processing, RCA International Service Corporation, Missile Test Project, Patrick Air Force Base, Florida. RCA International Service Corporation is subcontractor of the ETR Range Contractor, Pan American World Airways, Aerospace Services Division, Patrick Air Force Base, Florida, contract No. F08606-68-C-0040.

The sponsoring agency is Instrumentation Systems Analysis Branch, Instrumentation and Data Processing Division, Directorate of Range Operations, AFETR, Patrick Air Force Base, Florida. The Project Officer for this report is Mr. Hector Silvestre.

Grateful acknowledgement is given to members of the Real Time Computer System, In-Flight Analysis and Programming and Down Range Analysis and Programming units. In particular, appreciation is expressed to Mr. Wayne Miller and Mr. Dave Frank for making important analytical contributions and to Mrs. Jacque Thees for typing the report.

This technical report has been reviewed and approved.

Robert W. Schmeling
Lt. Colonel, USAF
Chief, Instrumentation and Data Processing Division
Directorate of Range Operations

TABLE OF CONTENTS

	<u>Page</u>
I. Introduction	1
II. Secular Variations	3
III. Periodic Variations.	9
III.1 Introduction.	9
III.2 Kozai Periodic Variations	9
III.3 Frazer Periodic Variations.	18
III.3.1 Introduction	18
III.3.2 Frazer Long Period Variations.	20
III.3.3 Frazer Short Period Variations	28
III.4 Inverse Computations.	36
IV. Applications	39
IV.1 Introduction	39
IV.2 Trajectory Generation.	39
IV.3 Orbit Determination.	49
Appendix I. Space Defense Center 5-Card Bulletin.	55
Appendix II. Subroutine DTPDA.	57
Appendix III. Subroutine ELRAT.	61
Appendix IV. Subroutine DELTA.	65
Appendix V. Subroutine DELXYZ	69
Appendix VI. Subroutine OSMCE.	73
Appendix VII. Subroutine UPDAT.	77
References	81

TABLES

	<u>Page</u>
I. Comparisons of SDC and Analytically Computed Secular Variations	7
II. Theoretical Trajectory Initial Conditions.	13
III. Theoretical Trajectory Gravity Model	14
IV. Examples of Errors Caused by Using Approximate Long Period Variations	27
V. Examples of Errors Caused by Using Approximate Short Period Variations.	35
VI. Example of Frazer Inverse Computations	37
VII. Theoretical Trajectory Initial Conditions.	43
VIII. Theoretical Mean Elements and Rates.	44
IX. Vacuum Trajectory Differences	45
X. Drag Trajectory Differences (Polynomial Update).	46
XI. Drag Trajectory Differences (Logarithmic Update)	48
XII. CASS Single-Pass Mean Elements for Orbit Determination.	50
XIII. CASS Polynomial Mean Element Residuals	51
XIV. CASS Polynomial and Analytical Orbit Solutions	52
XV. CASS Analytical Bulletin Prediction Errors	53

FIGURES

	<u>Page</u>
1. Kozai Semi-Major Axis Short Period Variations	15
2. Kozai Eccentricity Short Period Variations.	15
3. Kozai Inclination Short Period Variations	16
4. Kozai Argument of Perigee Short Period Variations	16
5. Kozai Right Ascension of Ascending Node Short Period Variations	17
6. Kozai Mean Anomaly Short Period Variations.	17
7. Frazer Semi-Major Axis Long Period Variations	23
8. Frazer Eccentricity Long Period Variations.	23
9. Frazer Inclination Long Period Variations	24
10. Frazer Argument of Perigee Long Period Variations	24
11. Frazer Right Ascension of Ascending Node Long Period Variations	25
12. Frazer Mean Anomaly Long Period Variations.	25
13. Frazer Mean Longitude Long Period Variations.	26
14. Frazer Semi-Major Axis Short Period Variations.	31
15. Frazer Eccentricity Short Period Variations	31
16. Frazer Inclination Short Period Variations.	32
17. Frazer Argument of Perigee Short Period Variations.	32
18. Frazer Right Ascension of Ascending Node Short Period Variations	33
19. Frazer Mean Anomaly Short Period Variations	33
20. Frazer Mean Longitude Short Period Variations	34

SECTION I

INTRODUCTION

If the gravity field of a homogeneous spherical earth were the only force acting on an object, the classical Keplerian orbital elements describing the size, shape and orientation of the orbit of the object would remain constant in time. However, the presence of various perturbative forces causes the classical (osculating) elements to vary with time. These variations can be divided into three categories: secular, short period and long period. The short period variations appear to be functions of the position of the object in its orbit. The long period variations appear to be functions of the position of perigee in space. Keplerian elements from which the short and long period variations have been removed are referred to herein as mean elements. The mean elements change monotonically with time and the rates of these changes are the secular variations.

Analysts making decisions concerning orbits of various objects must be aware of the fact that Keplerian elements vary with time. For example, if comparisons are desired among orbit determination solutions at various epochs, these comparisons must be made in mean elements. If classical elements are used, it may be erroneously inferred that a maneuver had occurred or that one or another solution was unreliable. Since mean elements are well behaved in time, mean elements at any epoch can be computed from those at any other epoch if the secular variations are known. However, it must be remembered that the mean elements do not represent the actual position of an object. For example, if observation station look angles are desired, they must be computed from osculating elements. Hence, it is necessary to be able to convert back and forth between mean and osculating elements.

In summary, the classical elements represent the actual position and velocity of the object but are poorly behaved in time. The mean elements do not represent the actual position and velocity but are well behaved in time. Since each of these characteristics is useful in orbit support, some means of transformation from one to the other is desired. The following sections give the equations for these transformations and show examples of their applications to both theoretical and real data.

The Keplerian elements used in this discussion are defined by:

- a = semi-major axis
- e = eccentricity
- i = inclination
- ω = argument of perigee
- Ω = right ascension of ascending node
- M = mean anomaly

The symbols for the classical elements are those used above, while the symbols for the equivalent mean elements are those above in conjunction with a bar superscript (e.g. \bar{a}).

It is not the purpose of this report to derive all the mathematical expressions used for the various computations, but rather to show what the computational procedures are, together with numerical results obtained. The references are recommended for derivations of the techniques. This report shows examples of the practical applications of these techniques.

SECTION II

SECULAR VARIATIONS

When using mean elements for orbit support it is necessary to have the secular variations or rates of change of these elements with time. Often when mean elements are obtained from an outside agency, the secular variations are included in the transmitted information. A typical example of this case is the Space Defense Center (SDC) 5-card bulletin, an example of which is shown in Appendix I. This bulletin has been recognized as a useful technique for transmitting orbital information and now enjoys wide-spread use over the Air Force Eastern Test Range (AFETR).

When secular rates are not furnished with the mean elements, or when the mean elements have been derived internally, it is necessary to be able to compute these rates as accurately as possible. This can be accomplished analytically if the equations are known or numerically if mean elements at several different epochs are available. The analytical technique will be discussed here, while the numerical is discussed in Section IV.3. The analytical secular rates are computed as functions of the earth's second zonal gravity harmonic coefficient, J_2 , and atmospheric drag.

The secular variation of the mean mean anomaly is the mean mean motion. This (perturbed by Kozai's factor) is given by (Ref. 1):

$$\bar{n} = \left\{ \frac{\mu_e}{\bar{a}^3} \left[1 - \frac{3}{2} J_2 a_e^2 \frac{(1-\bar{e}^2)^{\frac{1}{2}}}{\bar{p}^2} \left(1 - \frac{3}{2} \sin^2 \bar{i} \right) \right] \right\}^{\frac{1}{2}} \quad (\text{II.1})$$

where \bar{p} is the mean semi-latus rectum given by:

$$\bar{p} = \bar{a} (1-\bar{e}^2)$$

The rates of change of the mean argument of perigee and right ascension of ascending node are given by (Ref. 2 and 3):

$$\dot{\omega} = \frac{3\bar{n} J_2 a_e^2 (5 \cos^2 \bar{i} - 1)}{4\bar{p}^2} \quad (\text{II.2})$$

$$\dot{\Omega} = - \frac{3\bar{n} J_2 a_e^2 \cos \bar{i}}{2\bar{p}^2} \quad (\text{II.3})$$

The rate of change of the mean inclination is assumed to be zero. All element rates are mean element rates.

$$\frac{\ddot{e}}{2} = \left[\frac{\ddot{a}}{2} \right] \frac{1+\bar{e}}{\bar{a}} \quad (\text{II.12})$$

$$\frac{\ddot{n}}{6} = - \frac{3\bar{n} \left[\frac{\ddot{a}}{2} \right] + 5\dot{a} \left[\frac{\dot{n}}{2} \right]}{6\bar{a}} \quad (\text{II.13})$$

where

$$c = \frac{\dot{n}}{2} \frac{1}{\bar{n}}$$

$$d = Ac^2 \left[1 + \frac{n_0}{3(n_0 - \bar{n})} \right]$$

where

$$n_0 = 16.667 \text{ revs/day}$$

$$A = 0, \text{ if } \bar{e} \geq 0.06$$

$$A = 4, \text{ if } \bar{e} < 0.06 \text{ and } \bar{n} \leq 16.204$$

$$A = 13, \text{ if } \bar{e} < 0.06 \text{ and } \bar{n} > 16.204$$

Thus, the mean element secular variations can be obtained analytically for whatever use may be desired of them. The capabilities of this technique can be demonstrated by attempting to reproduce the element rates appearing on a SDC 5-card bulletin. The results of such a test are shown in Table I. The six mean elements a and \dot{a} were input and the other rates were computed from them. Notice the difference between SDC and analytical values for $\frac{\ddot{a}}{2}$ and $\frac{\ddot{e}}{2}$. Drag effects should cause negative rather than positive values.

Analytical secular variations are used for trajectory generation in Section IV.2 where it is shown that better results are obtained when $\frac{\ddot{a}}{2}$, $\frac{\ddot{e}}{2}$, $\frac{\ddot{w}}{2}$, and $\frac{\ddot{n}}{6}$ are zero for that particular example. It could be that these terms are necessary for use with objects more significantly affected by drag. In any case, it is probably true that the empirical expression for $\frac{\ddot{a}}{2}$ could be improved. Analytically and numerically computed secular ² variations are compared in Section IV.3. Appendix III shows the FORTRAN coding for computing all the secular rates described above. All cases studied have shown that best results are obtained with the above-mentioned acceleration terms set to zero.

TABLE I
COMPARISONS OF SDC AND ANALYTICALLY COMPUTED
SECULAR VARIATIONS

<u>Parameter</u>	SDC Object #4483 <u>Bulletin #28</u>	<u>Analytical</u>
\bar{a} (earth radii)	1.06351376	Input
\bar{e}	.032704	Input
\bar{i} (deg)	48.3932	Input
$\bar{\omega}$ (deg)	129.4386	Input
$\bar{\Omega}$ (deg)	247.0671	Input
\bar{M} (deg)	233.5949	Input
$\dot{\bar{a}}$ (ER/day)	- 1.157451x10 ⁻³	Input
$\frac{\dot{\bar{a}}}{2}$ (ER/day ²)	1.574609x10 ⁻⁶	- 3.198782x10 ⁻⁵
$\dot{\bar{e}}$	- 1.0527x10 ⁻³	- 1.0527x10 ⁻³
$\frac{\dot{\bar{e}}}{2}$	2.8643x10 ⁻⁷	- 2.9094x10 ⁻⁵
$\dot{\bar{i}}$ (deg/day)	0.	0.
$\dot{\bar{\omega}}$ (deg/day)	4.84710	4.84601
$\frac{\dot{\bar{\omega}}}{2}$ (deg/day ²)	8.8975x10 ⁻³	8.8955x10 ⁻³
$\dot{\bar{\Omega}}$ (deg/day)	- 5.34388	- 5.34265
$\frac{\dot{\bar{\Omega}}}{2}$ (deg/day ²)	- 9.8094x10 ⁻³	- 9.8072x10 ⁻³
$\dot{\bar{n}}$ (rev/day)	15.53805068	15.53797780
$\frac{\dot{\bar{n}}}{2}$ (rev/day ²)	1.2682872x10 ⁻²	1.268280x10 ⁻²
$\frac{\dot{\bar{n}}}{6}$ (rev/day ³)	0.	2.45174 x10 ⁻⁴
$\frac{\dot{\bar{n}}}{24}$ (rev/day ⁴)	0.	0.

SECTION III

PERIODIC VARIATIONS

III.1 Introduction

The short and long period variations in the classical Keplerian elements can be approximated as functions of the earth's second and third zonal gravity harmonic coefficients. Two methods for computing the short period variations have been used at the AFETR Real Time Computer System (RTCS), one developed by Y. Kozai (Ref 5) and the other by J. B. Frazer (Ref 7). The Frazer method has also been used to compute long period variations. The two methods are presented below along with discussions of their applicability.

III.2 Kozai Periodic Variations

This method has been used at the RTCS to compute short period variations in the Keplerian elements as functions of the earth's second zonal gravity harmonic and is valid for elliptical orbits only. This method computes the short period variations from the mean elements.

First the eccentric anomaly is computed by solving Kepler's equation iteratively:

$$\begin{aligned}\bar{E}^1 &= \bar{M} && \text{on first iteration} \\ \bar{E} &= \bar{E}^1 - \frac{\bar{E}^1 - \bar{e} \sin \bar{E}^1 - \bar{M}}{1 - \bar{e} \cos \bar{E}^1} && \text{on succeeding iterations}\end{aligned}$$

The process is converged when two successive estimates are within some epsilon of each other. Then the true anomaly is given by

$$\bar{v} = 2 \tan^{-1} \left[\left[\frac{1+\bar{e}}{1-\bar{e}} \right]^{\frac{1}{2}} \frac{\sin \left(\frac{\bar{E}}{2} \right)}{\cos \left(\frac{\bar{E}}{2} \right)} \right]$$

The mean radius from the center of the earth to the object is given by:

$$\bar{r} = \bar{a}(1 - \bar{e} \cos \bar{E})$$

and the mean semi-latus rectum is given by:

$$\bar{p} = \bar{a}(1 - \bar{e}^2)$$

Kozai applies an extra perturbation to the mean semi-major axis in order to satisfy the following relationship:

$$\bar{n}^2 \bar{a}^3 = \mu_e \left[1 - \frac{3J_2 a_e^2}{2\bar{p}^2} \left[1 - \frac{3}{2} \sin^2 \bar{i} \right] \left[1 - \bar{e}^2 \right]^{\frac{1}{2}} \right]$$

where a_e = earth's semi-major axis
 μ_e = earth's gravity constant

and \bar{n} is the mean mean motion. When computing osculating from mean elements, first the extra perturbation is removed then the short period variations are computed and added to the mean elements. The perturbed mean semi-major axis is given by:

$$\bar{a}^1 = \frac{\bar{a}}{1 - \frac{3J_2 a_e^2}{2\bar{p}^2} \left[1 - \frac{3}{2} \sin^2 \bar{i} \right] \left[1 - \bar{e}^2 \right]^{\frac{1}{2}}} \quad (\text{III.1})$$

Then the short period Keplerian element variations are given by (Ref 1):

$$\delta a_s = \frac{J_e}{\bar{a}} \left\{ \frac{2}{3} \left[1 - \frac{3}{2} \sin^2 \bar{i} \right] \left[\left(\frac{\bar{a}}{\bar{r}} \right)^3 - (1 - \bar{e}^2)^{-\frac{3}{2}} \right] + \left(\frac{\bar{a}}{\bar{r}} \right)^3 \sin^2 \bar{i} \cos 2 (\bar{v} + \bar{\omega}) \right\} \quad (\text{III.2})$$

$$\begin{aligned} \delta e_s = & \frac{1 - \bar{e}^2}{\bar{e}} \left(\frac{J_e}{\bar{a}^2} \right) \left\{ \frac{1}{3} \left[1 - \frac{3}{2} \sin^2 \bar{i} \right] \left[\left(\frac{\bar{a}}{\bar{r}} \right)^3 - (1 - \bar{e}^2)^{-\frac{3}{2}} \right] + \frac{1}{2} \left(\frac{\bar{a}}{\bar{r}} \right)^3 \sin^2 \bar{i} \cos 2 (\bar{v} + \bar{\omega}) \right\} \\ & - \frac{\sin^2 \bar{i}}{2\bar{e}} \left(\frac{J_e}{\bar{a}\bar{p}} \right) \left\{ \cos 2 (\bar{v} + \bar{\omega}) + \bar{e} \cos (\bar{v} + 2\bar{\omega}) + \frac{1}{3} \bar{e} \cos (3\bar{v} + 2\bar{\omega}) \right\} \end{aligned} \quad (\text{III.3})$$

$$\begin{aligned} \delta i_s = & \frac{J_e}{\bar{p}^2} \sin^2 \bar{i} \left[\cos 2 (\bar{v} + \bar{\omega}) + \bar{e} \cos (\bar{v} + 2\bar{\omega}) + \frac{\bar{e}}{3} \cos (3\bar{v} + 2\bar{\omega}) \right] \end{aligned} \quad (\text{III.4})$$

$$\begin{aligned}
\delta\omega_s = -\frac{J_e}{p^2 e} \left\{ \bar{e} \left(2 - \frac{5}{2} \sin^2 \bar{i} \right) (\bar{v} - \bar{M} + \bar{e} \sin \bar{v}) \right. \\
+ \left(1 - \frac{3}{2} \sin^2 \bar{i} \right) \left[\left(1 - \frac{\bar{e}^2}{4} \right) \sin \bar{v} + \frac{\bar{e}}{2} \sin 2\bar{v} \right. \\
+ \left. \left. \frac{\bar{e}^2}{12} \sin 3\bar{v} \right] \right. \\
- \sin(\bar{v} + 2\bar{\omega}) \left[\frac{1}{4} \sin^2 \bar{i} + \bar{e}^2 \left(\frac{1}{2} - \frac{15}{16} \sin^2 \bar{i} \right) \right] \\
+ \frac{\bar{e}^2}{16} \sin^2 \bar{i} \sin(\bar{v} - 2\bar{\omega}) - \frac{\bar{e}}{2} \left(1 - \frac{5}{2} \sin^2 \bar{i} \right) \sin 2(\bar{v} + \bar{\omega}) \\
+ \sin(3\bar{v} + 2\bar{\omega}) \left[\frac{7}{12} \sin^2 \bar{i} - \frac{\bar{e}^2}{6} \left(1 - \frac{19}{8} \sin^2 \bar{i} \right) \right] \\
+ \left. \left. \frac{3\bar{e}}{8} \sin^2 \bar{i} \sin(4\bar{v} + 2\bar{\omega}) + \frac{\bar{e}^2}{16} \sin^2 \bar{i} \sin(5\bar{v} + 2\bar{\omega}) \right] \right\} \quad (\text{III.5})
\end{aligned}$$

$$\begin{aligned}
\delta\Omega_s = -\frac{J_e}{p^2} \cos \bar{i} \left[(\bar{v} - \bar{M} + \bar{e} \sin \bar{v}) - \frac{1}{2} \sin 2(\bar{v} + \bar{\omega}) \right. \\
- \left. \frac{\bar{e}}{2} \sin(\bar{v} + 2\bar{\omega}) - \frac{\bar{e}}{6} \sin(3\bar{v} + 2\bar{\omega}) \right] \quad (\text{III.6})
\end{aligned}$$

$$\begin{aligned}
\delta M_s = -\frac{J_e}{p^2 \bar{e}} (1 - \bar{e}^2) \left\{ \left(1 - \frac{3}{2} \sin^2 \bar{i} \right) \left[\left(1 - \frac{\bar{e}^2}{4} \right) \sin \bar{v} \right. \right. \\
+ \left. \frac{\bar{e}}{2} \sin 2\bar{v} + \frac{\bar{e}^2}{12} \sin 3\bar{v} \right] \\
+ \sin^2 \bar{i} \left[\frac{1}{4} \left(1 + \frac{5\bar{e}^2}{4} \right) \sin(\bar{v} + 2\bar{\omega}) - \frac{\bar{e}^2}{16} \sin(\bar{v} - 2\bar{\omega}) \right. \\
- \frac{7}{12} \left(1 - \frac{\bar{e}^2}{28} \right) \sin(3\bar{v} + 2\bar{\omega}) - \frac{3\bar{e}}{8} \sin(4\bar{v} + 2\bar{\omega}) \\
- \left. \left. \frac{\bar{e}^2}{16} \sin(5\bar{v} + 2\bar{\omega}) \right] \right\} \quad (\text{III.7})
\end{aligned}$$

$$\text{where } J_e = \frac{3}{2} J_2 a_e^2$$

Notice that in the above expressions for $\delta\omega_s$ and δM_s there are eccentricity divisors. The variations in these elements are undefined for circular orbits because the elements themselves are undefined.

These variations are added to the mean elements to yield quasi-osculating (short period variations only).

Appendix IV gives the FORTRAN coding for this algorithm and Figures 1 through 6 show theoretical results obtained by the method. The figures show the classical Keplerian elements and quasi mean elements (short period variations removed) for one orbital revolution of a satellite. An orbit was numerically generated with initial conditions in the classical elements given in Table II, with no drag and using the gravity model shown in Table III. The Kozai algorithm was applied to points taken from the theoretical trajectory at five minute intervals. In this case osculating elements were being transformed to quasi mean elements. Since the variation equations are functions of the mean elements, the solution was performed iteratively. Secular variations in the elements were removed for ease of plotting.

Due to the problems of this algorithm associated with near circular orbits, this method is not recommended for general orbit support.

The effect of Kozai's extra perturbation can be seen in Figure 1, where the quasi mean is displaced from the center of the plot of the osculating semi-major axis.

TABLE II
THEORETICAL TRAJECTORY INITIAL CONDITIONS

Classical Keplerian Elements

$a = 22981800.$ feet

$e = .02$

$i = 28.$ deg

$\omega = 9.$ deg

$\Omega = 115.$ deg

$M = 0.$ deg

TABLE III
THEORETICAL TRAJECTORY GRAVITY MODEL

$$a_e = 6378.165 \text{ km}$$

$$\mu_e = 398601.2 \text{ km}^3/\text{sec}^2$$

<u>n</u>	<u>m</u>	<u>C_{nm}</u> [*]	<u>S_{nm}</u> [*]
2	0	-1082.3	0
3	0	2.3	0
4	0	1.8	0
2	1	0	0
2	2	1.68	-0.64
3	1	1.77	0.19
3	2	0.29	-0.03
3	3	0.15	0.14
4	1	-0.57	-0.46
4	2	0.06	0.26
4	3	0.08	-0.003
4	4	-0.008	0.006

*Multiply all values shown by 10^{-6}

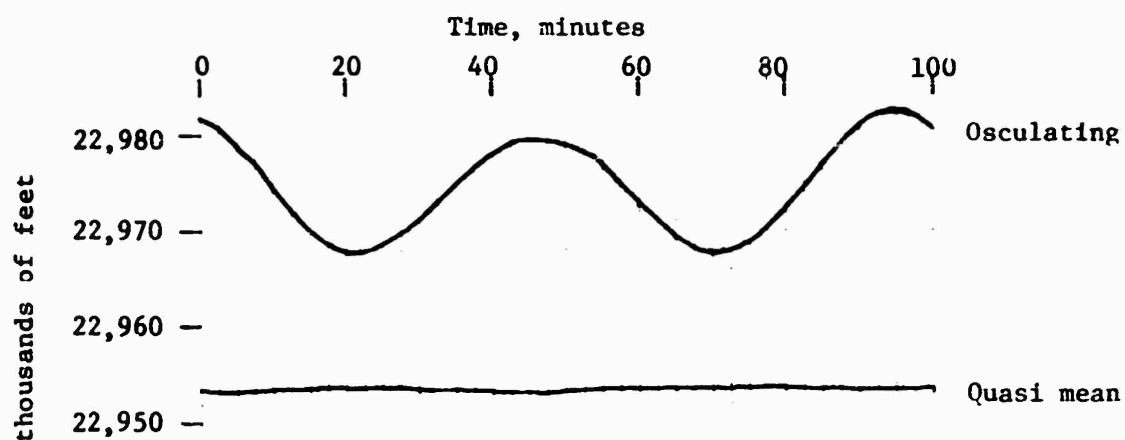


Figure 1. Kozai Semi-Major Axis Short Period Variations

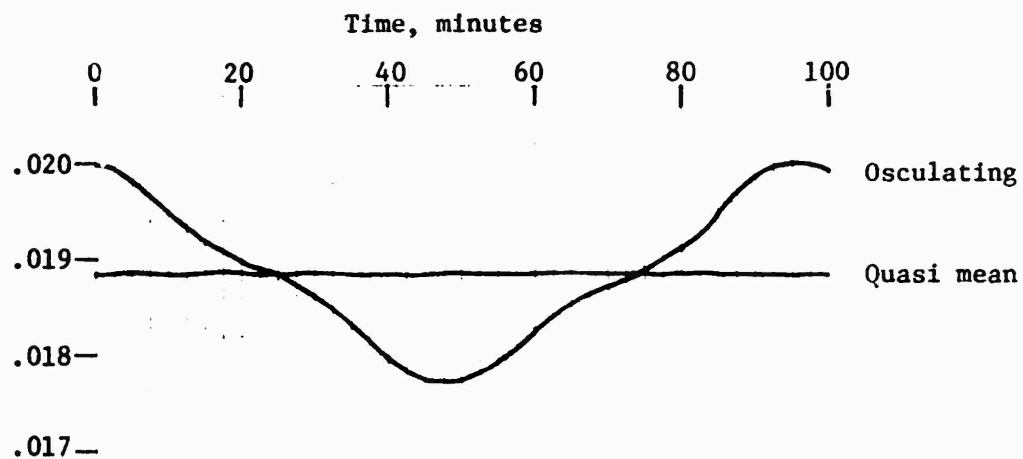


Figure 2. Kozai Eccentricity Short Period Variations

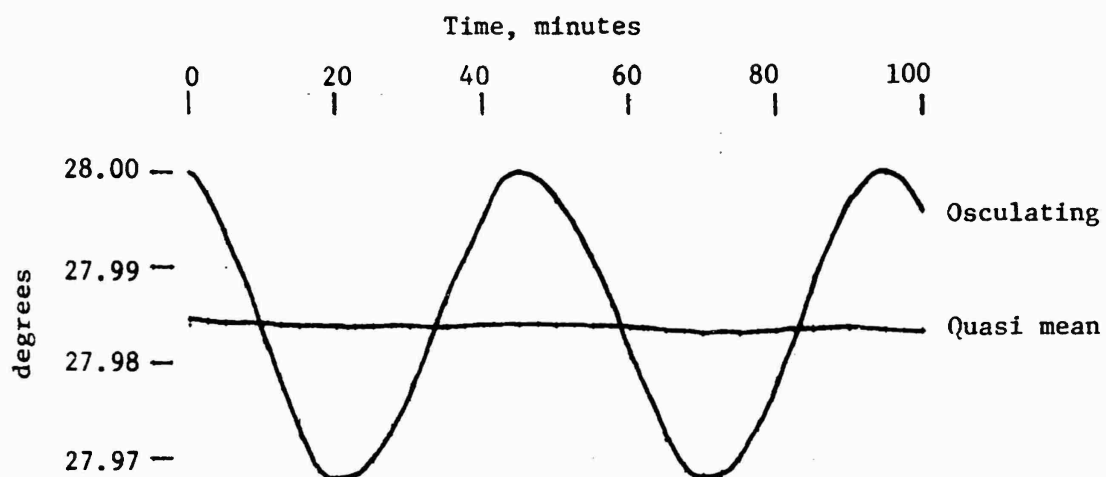


Figure 3. Kozai Inclination Short Period Variations

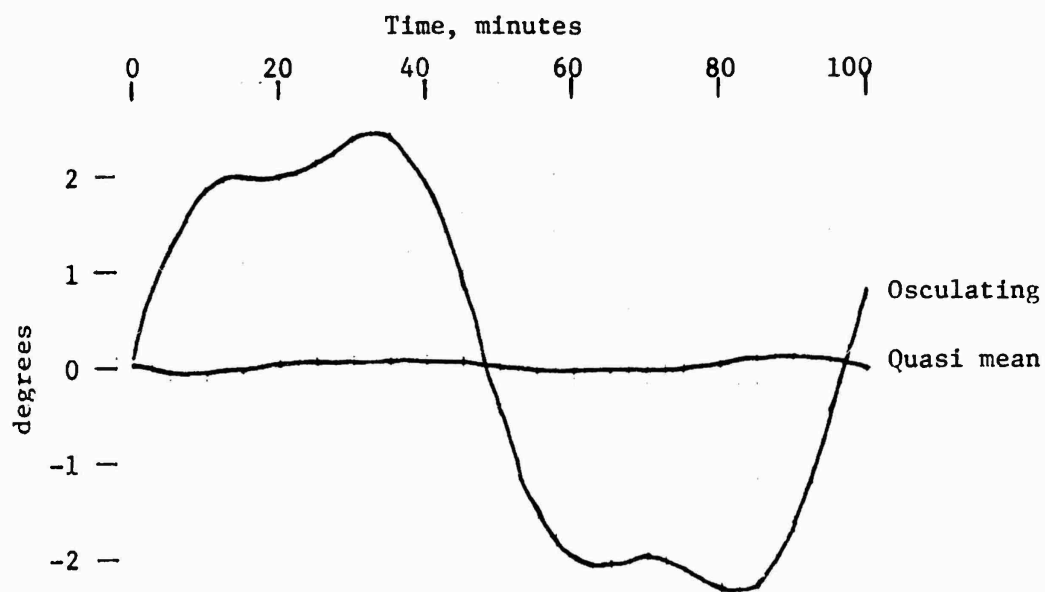


Figure 4. Kozai Argument of Perigee Short Period Variations

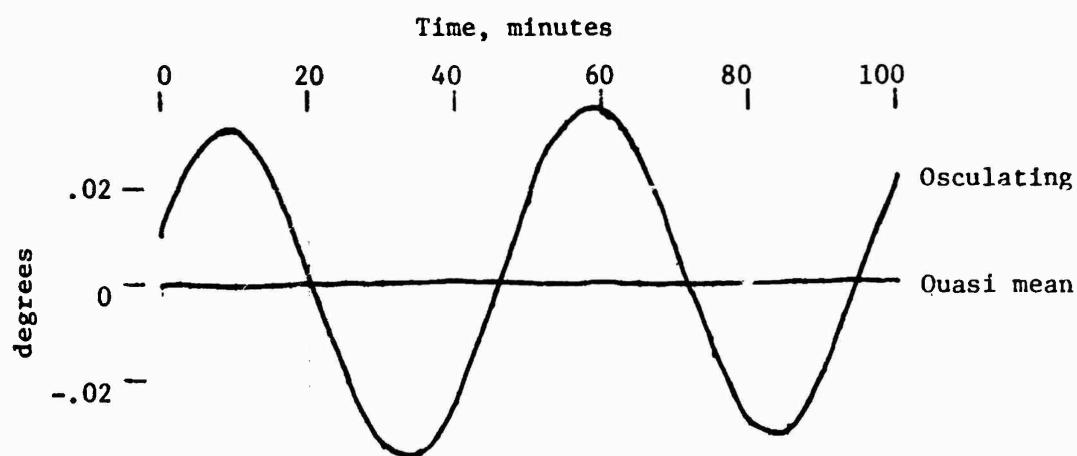


Figure 5. Kozai Right Ascension of Ascending Node Short Period Variations

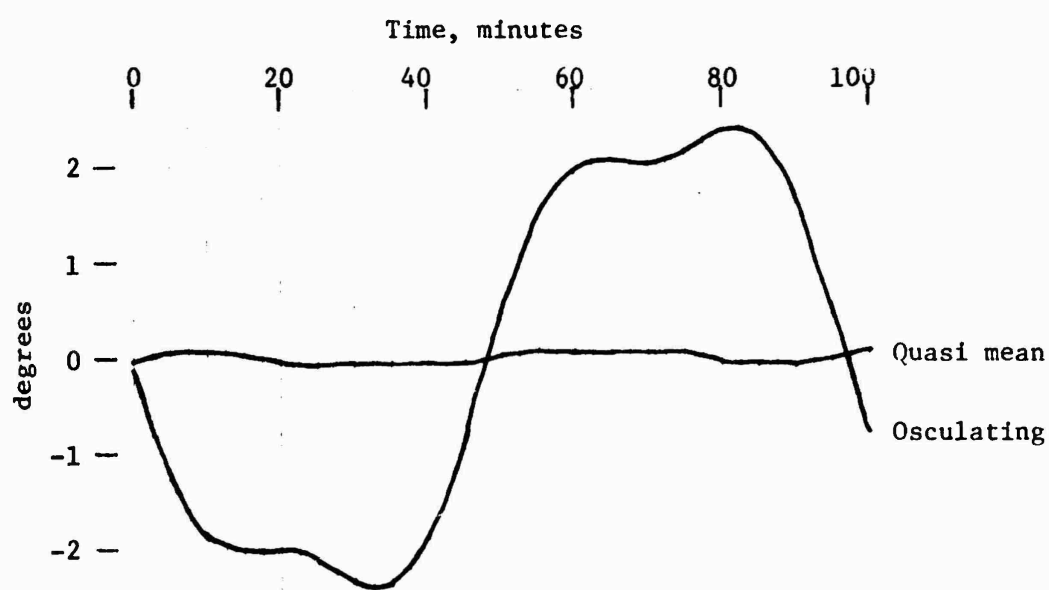


Figure 6. Kozai Mean Anomaly Short Period Variations

III.3 Frazer Periodic Variations

III.3.1 Introduction

The method developed by J. B. Frazer (Ref. 7) does not have a problem with circular orbits as does the Kozai because the variations are computed in Cartesian elements. This method is valid for circular and elliptical orbits only and as described herein is invalid for equatorial orbits due to sine inclination divisors.

First, the mean Keplerian elements are transformed to mean Cartesian elements as follows:

$$\begin{aligned}\vec{r} &= \bar{r} \vec{U} \\ \dot{\vec{r}} &= \dot{\bar{r}} \vec{U} + \bar{r} \dot{\vec{V}}\end{aligned}$$

where

$$\vec{r} = \begin{bmatrix} \bar{x} \\ \bar{y} \\ \bar{z} \end{bmatrix}, \quad \dot{\vec{r}} = \begin{bmatrix} \dot{\bar{x}} \\ \dot{\bar{y}} \\ \dot{\bar{z}} \end{bmatrix}$$

The osculating Cartesian system is defined as follows: x, y, z are position components in an inertial geocentric righthanded system with x and y in the plane of the mean equator of date, x toward the mean Vernal equinox of date, and z toward the north pole ("mean" here refers to the absence of nutations).

$$\begin{aligned}\vec{U} = \begin{bmatrix} U_x \\ U_y \\ U_z \end{bmatrix} &= \begin{bmatrix} \cos \bar{u} \cos \bar{\Omega} - \sin \bar{u} \sin \bar{\Omega} \cos \bar{i} \\ \cos \bar{u} \sin \bar{\Omega} + \sin \bar{u} \cos \bar{\Omega} \cos \bar{i} \\ \sin \bar{u} \sin \bar{i} \end{bmatrix} \\ \vec{V} = \begin{bmatrix} V_x \\ V_y \\ V_z \end{bmatrix} &= \begin{bmatrix} -\sin \bar{u} \cos \bar{\Omega} - \cos \bar{u} \sin \bar{\Omega} \cos \bar{i} \\ -\sin \bar{u} \sin \bar{\Omega} + \cos \bar{u} \cos \bar{\Omega} \cos \bar{i} \\ \cos \bar{u} \sin \bar{i} \end{bmatrix}\end{aligned}$$

where \bar{u} = mean argument of latitude = $\bar{\omega} + \bar{v}$ and where \bar{r} is the radius from the earth's center to the object given by

$$r = \frac{\bar{p}}{1 + \bar{e} \cos \bar{v}}$$

$\dot{\bar{r}}$ is the rate of change of \bar{r} given by

$$\dot{\bar{r}} = \left[\frac{\mu_e}{\bar{p}} \right]^{1/2} \bar{e} \sin \bar{v}$$

and $\bar{r}\dot{v}$ is the product of the radius and the true anomaly rate of change given by

$$\bar{r}\dot{v} = \left[\frac{\mu}{p} \right]^{\frac{1}{2}} (1 + \bar{e} \cos \bar{v})$$

where \bar{p} = mean semi-latus rectum = $\bar{a}(1 - \bar{e}^2)$

The perturbed or osculating Cartesian vector due to short and long period variations is given by

$$\vec{r} = (\bar{r} + \delta r) (\vec{U} + \delta \vec{U})$$

$$\vec{r} = (\bar{r} + \delta r) (\vec{U} + \delta \vec{U}) + (\bar{r}\dot{v} + \delta r\dot{v}) (\vec{V} + \delta \vec{V})$$

or the variations alone are given by

$$\delta \vec{r} = \delta r \vec{U} + \bar{r} \delta \vec{U}$$

$$\delta \vec{r} = \delta r \vec{U} + \delta r \dot{v} \vec{V} + \bar{r} \delta \vec{U} + \bar{r} \dot{v} \delta \vec{V}$$

Using

$$\vec{W} = \vec{U}_x \vec{V} = \begin{bmatrix} W_x \\ W_y \\ W_z \end{bmatrix} = \begin{bmatrix} \sin \bar{\Omega} \sin \bar{I} \\ -\cos \bar{\Omega} \sin \bar{I} \\ \cos \bar{I} \end{bmatrix}$$

then

$$\delta \vec{U} = (\delta u + \delta \Omega \cos \bar{I}) \vec{V} + (\delta i \sin \bar{u} - \delta \Omega \cos \bar{u} \sin \bar{I}) \vec{W}$$

$$\delta \vec{V} = -(\delta u + \delta \Omega \cos \bar{I}) \vec{U} + (\delta i \cos \bar{u} + \delta \Omega \sin \bar{u} \sin \bar{I}) \vec{W}$$

and hence

$$\delta \vec{r} = \delta r \vec{U} + \bar{r} (\delta u + \delta \Omega \cos \bar{I}) \vec{V} + \bar{r} (\delta i \sin \bar{u} - \delta \Omega \cos \bar{u} \sin \bar{I}) \vec{W}$$

$$\begin{aligned} \delta \vec{r} = & \left[\delta r - \bar{r} \dot{v} (\delta u + \delta \Omega \cos \bar{I}) \right] \vec{U} \\ & + \left[\delta r \dot{v} + \bar{r} (\delta u + \delta \Omega \cos \bar{I}) \right] \vec{V} \\ & + \left[\bar{r} (\delta i \sin \bar{u} - \delta \Omega \cos \bar{u} \sin \bar{I}) \right. \\ & \left. + \bar{r} \dot{v} (\delta i \cos \bar{u} + \delta \Omega \sin \bar{u} \sin \bar{I}) \right] \vec{W} \end{aligned}$$

These variations are composed of short and long period components as

$$\delta \vec{r} = \delta \vec{r}_s + \delta \vec{r}_L$$

$$\delta \vec{r} = \delta \vec{r}_s + \delta \vec{r}_L$$

which are computed separately as shown in the following sections. Once the short and long period variations have been computed, osculating Cartesian elements can be obtained. The osculating Cartesian elements can then be transformed into osculating Keplerian elements by standard techniques.

III.3.2 Frazer Long Period Variations

Although Frazer develops the variations in a Cartesian coordinate system, it is interesting to note the forms of the equations for the long period variations in the Keplerian elements (Ref. 7). For all zonal harmonics, J_n , $n > 2$:

$$\delta a_L = 0$$

$$\delta e_L = S_n (1 - \bar{e}^2) \sin \bar{I} \cos \lambda \xi$$

$$\delta i_L = -S_n \bar{e} \cos \bar{I} \cos \lambda \xi$$

$$\delta \omega_L = -S_n \bar{e} \sin \bar{I} \left[5 - 2n - \mu \frac{1 - \bar{e}^2}{\bar{e}^2} - \frac{10 \cos^2 \bar{I}}{1 - 5 \cos^2 \bar{I}} + \frac{v \cos^2 \bar{I}}{\sin^2 \bar{I}} \right] \frac{\sin \lambda \xi}{\lambda}$$

$$\delta \Omega_L = -S_n \bar{e} \sin \bar{I} \cos \bar{I} \left[\frac{10}{1 - 5 \cos^2 \bar{I}} - \frac{v}{\sin^2 \bar{I}} \right] \frac{\sin \lambda \xi}{\lambda}$$

$$\delta M_L = -S_n \frac{(1 - \bar{e}^2)^{3/2}}{\bar{e}} \sin \bar{I} \frac{\mu}{\lambda} \sin \lambda \xi$$

where

$$S_n = - \frac{8(n-1)!}{3 \cdot 2^n} \frac{J_n a^{n-2}}{J_2 \bar{p}^{n-2} (1 - 5 \cos^2 \bar{I})} \sum_{\lambda, \mu, \nu} Q$$

$$Q = \frac{(-1)^{\frac{n-\nu}{2}} (n+\nu)! \bar{e}^{\mu-1} \sin^{v-1} \bar{I}}{2^{\mu+\nu} \left(\frac{n-\nu}{2}\right)! \left(\frac{n+\nu}{2}\right)! \left(\frac{\nu-\lambda}{2}\right)! \left(\frac{\nu+\lambda}{2}\right)! (n-\mu-1)! \left(\frac{\mu-\lambda}{2}\right)! \left(\frac{\mu+\lambda}{2}\right)!}$$

$$\begin{aligned} \sin \lambda \xi &= -(-1)^{\frac{\lambda}{2}} \sin \lambda \bar{\omega}, \lambda \text{ even} \\ &= -(-1)^{\frac{\lambda-1}{2}} \cos \lambda \bar{\omega}, \lambda \text{ odd} \end{aligned}$$

$$\begin{aligned} \cos \lambda \xi &= (-1)^{\frac{\lambda}{2}} \cos \lambda \bar{\omega}, \lambda \text{ even} \\ &= (-1)^{\frac{\lambda-1}{2}} \sin \lambda \bar{\omega}, \lambda \text{ odd} \end{aligned}$$

$$\lambda = 2, 4, \dots, (n-2) , n \text{ even}$$

$$= 1, 3, \dots, (n-2) , n \text{ odd}$$

$$\mu = \lambda, \lambda+2, \dots, (n-2)$$

$$\nu = \lambda, \lambda+2, \dots, n$$

$$a_e = \text{earth's semi-major axis}$$

As can be seen in the above equations, there is no first order long period variation in the semi-major axis. Since there is an eccentricity multiplier in the expressions for the long period variations in inclination and right ascension of the ascending node, these variations are insignificant for near-circular orbits. There is also an eccentricity multiplier in S_n for all n except $n=3(J_3)$. For near-circular orbits, then, J_3 is the only zonal gravity harmonic coefficient which contributes significantly to long period variations, and then only in eccentricity, argument of perigee and mean anomaly. But argument of perigee, mean anomaly and their variations (note eccentricity divisors) are undefined for circular orbits.

In the above equation for S_n there is a divisor given as

$$1 - 5\cos^2 i$$

This expression becomes zero when inclination is approximately 63.5 or 116.5 degrees. This is known as the critical inclination. At the critical inclination the long period variations in the orbital elements are undefined.

After considerable manipulation, Frazer reduces the long period variations as functions of the zonal harmonic coefficient J_3 to the following in the inertial geocentric Cartesian elements (Ref. 7):

$$\delta \vec{r}_L = \bar{r} \alpha_2 \left[\sin \bar{i} (1 + \bar{e} \cos \bar{v}) \sin \bar{u} \vec{U} + \sin \bar{i} (2 + \bar{e} \cos \bar{v}) \cos \bar{u} \vec{V} + \cos \bar{i} \bar{e} \cos \bar{v} \vec{W} \right] \quad (\text{III.10})$$

$$\delta \vec{t}_L = -\left(\frac{\mu_e}{\bar{p}}\right)^{1/2} \alpha_2 \left[\sin \bar{i} (1 + \bar{e} \cos \bar{v}) \cos \bar{u} \vec{U} + \sin \bar{i} (\sin \bar{u} + \bar{e} \sin \bar{u}) \vec{V} + \cos \bar{i} \bar{e} \sin \bar{v} \vec{W} \right] \quad (\text{III.11})$$

where

$$\alpha_2 = \frac{J_3 a_e}{2J_2 \bar{p}}$$

Notice that in the expressions for the Cartesian variations due to J_3 , the effect of the critical inclination does not appear.

Appendix V gives the FORTRAN coding for the Frazer algorithm (includes short period variations) and Figures 7 through 13 show theoretical results obtained in the Keplerian elements by applying the long period variations as described above. The example used is the same as that previously given for the Kozai method in Tables II and III. The mean longitude variations, δL_L , given in Figure 13 are defined by:

$$\delta L_L = \delta \omega_L + \delta M_L$$

The figures show mean elements and quasi mean elements (short period variations removed) for twenty days of satellite motion. Secular variations were removed for ease of plotting.

Originally, long period variations due to J_2 and J_4 were included in the computations, but numerical results obtained when comparing trajectory generations via mean elements versus numerical integration (Section IV.2) were much poorer than those obtained with J_2 and J_4 effects eliminated.

If the computations of these variations are restricted to near-circular orbits, the above equations (with $\bar{e}=0$) reduce to:

$$\delta \vec{r}_L = \alpha_2 \bar{r} \sin \bar{i} (\sin \bar{u} \vec{U} + 2 \cos \bar{u} \vec{V})$$

$$\delta \vec{r}_L = -\alpha_2 \left(\frac{\mu_e}{p} \right)^{1/2} \sin \bar{i} (\cos \bar{u} \vec{U} + \sin \bar{u} \vec{V})$$

These are the resulting approximate equations even when J_2 and J_4 are included in the full equations.

These approximate equations yield long period variations with errors varying as a function of the eccentricity. Table IV shows some typical errors, encountered at various eccentricities, caused by using the approximate rather than the full equations. Since these are just isolated examples, they must not by any means be considered as maximum errors which could be obtained. The errors given are the differences between elements obtained after applying the equations III.10-11 and the approximate equations above to an input vector.

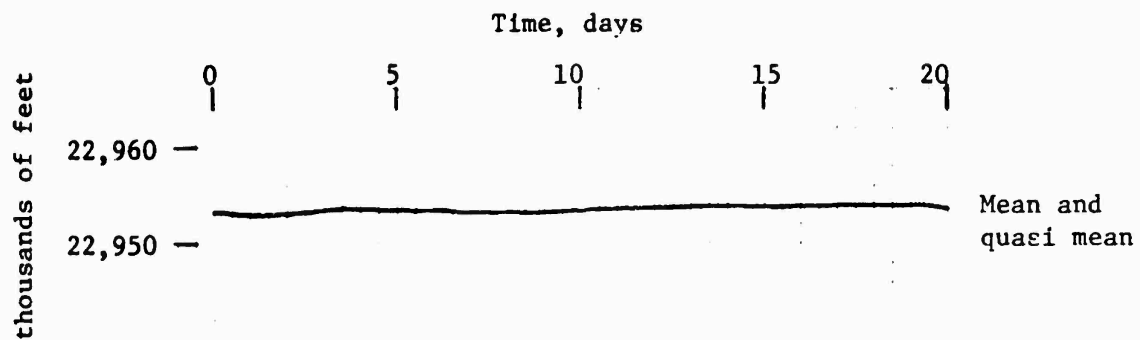


Figure 7. Frazer Semi-Major Axis Long Period Variations

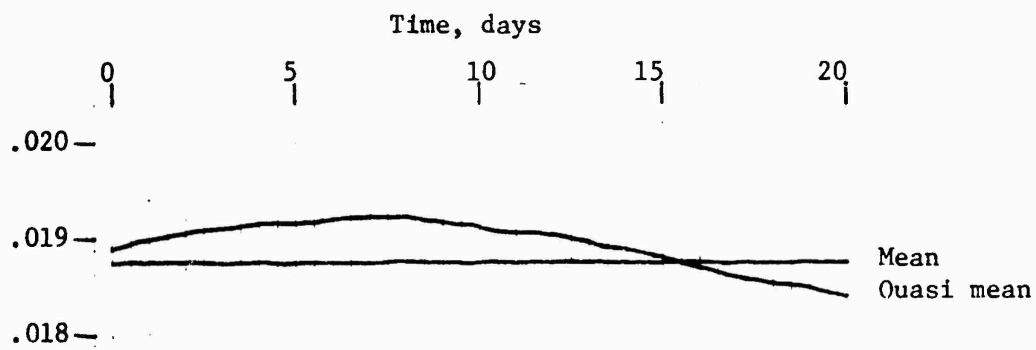


Figure 8. Frazer Eccentricity Long Period Variations

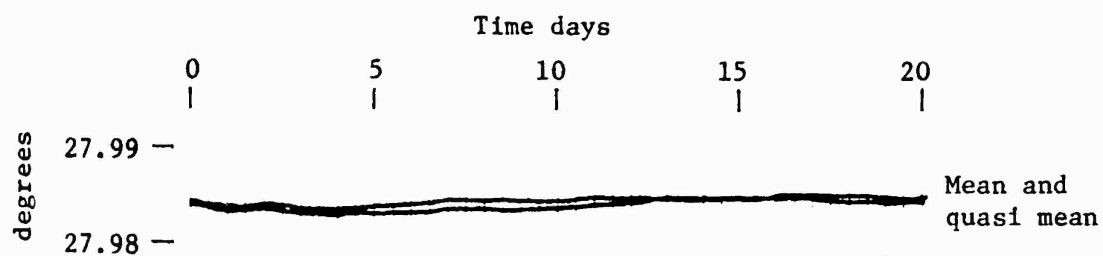


Figure 9. Frazer Inclination Long Period Variations

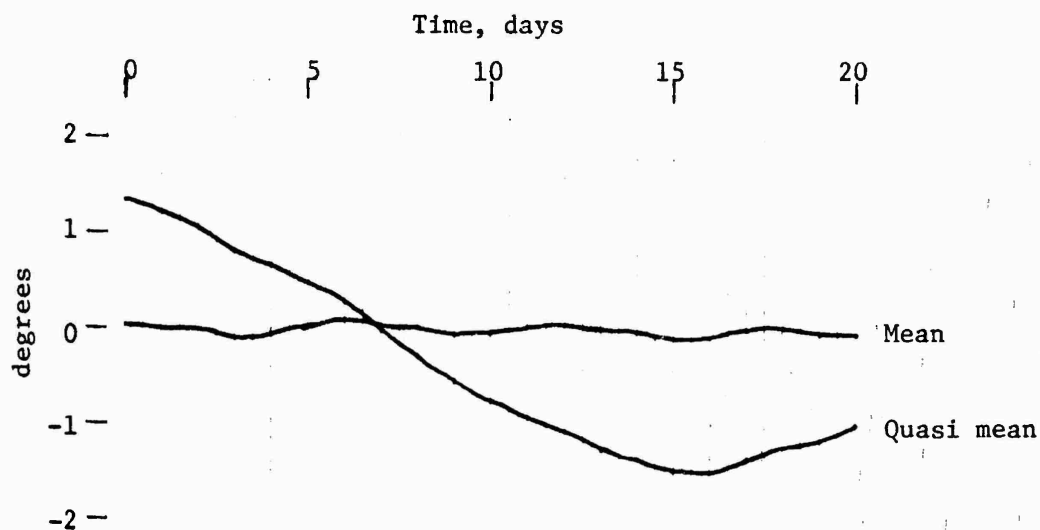


Figure 10. Frazer Argument of Perigee Long Period Variations

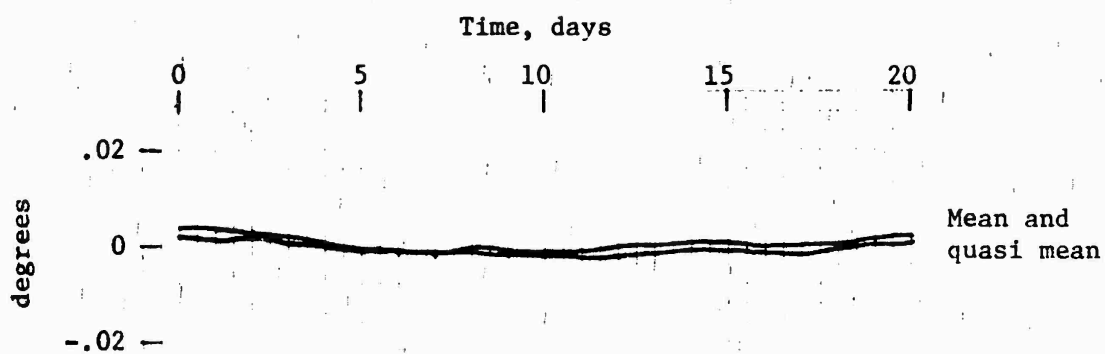


Figure 11. Frazer Right Ascension of Ascending Node Long Period Variations

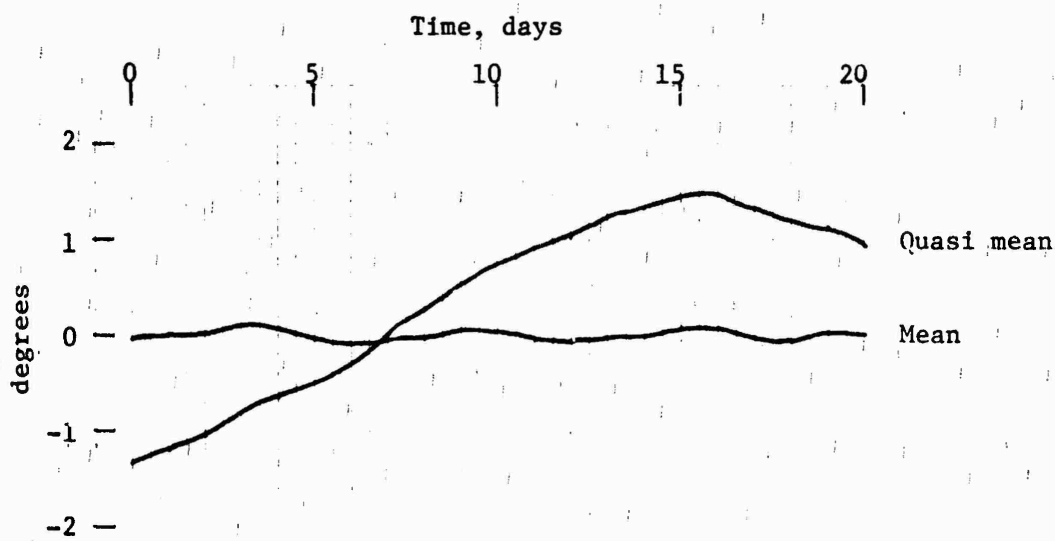


Figure 12. Frazer Mean Anomaly Long Period Variations

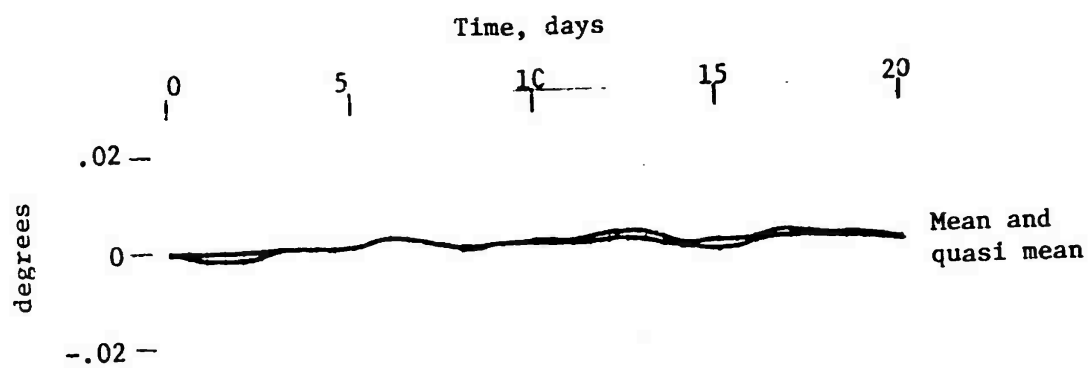


Figure 13. Frazer Mean Longitude Long Period Variations

TABLE IV

Examples of Errors Caused by Using
Approximate Long Period Variations

	Eccentricity		
	0.02	0.125	0.6
δx (ft.)	0.	0.	0.
δy (ft.)	0.	0.	0.
δz (ft.)	207.	1926.	7861.
$\dot{\delta x}$ (ft./sec.)	0.18	1.59	1.10
$\dot{\delta y}$ (ft./sec.)	0.04	0.44	0.19
$\dot{\delta z}$ (ft./sec.)	0.32	2.34	3.84
δa (ft.)	249.	2960.	7966.
δe	0.000004	0.000111	0.000010
δi (deg.)	0.0002	0.0023	0.0096
$\delta \omega$ (deg.)	0.0233	0.0421	0.0275
$\delta \Omega$ (deg.)	0.0019	0.0009	0.0332
δM (deg.)	0.0215	0.0382	0.0013

III.3.3 Frazer Short Period Variations

The short period variations are computed as functions of the earth's second gravity zonal harmonic coefficient in the elements \bar{r} , \bar{u} , $\bar{\Omega}$, \bar{I} , \bar{e} , $\bar{r}\bar{v}$, and then these variations are transformed to the inertial Cartesian system as shown in Section III.3.1. That is (Ref. 7):

$$\delta r_s = \alpha \bar{p} \left\{ \sin^2 \bar{I} \cos 2\bar{u} + (1-3\cos^2 \bar{I}) \left[1 - \frac{(1-\bar{e}^2)^{\frac{1}{2}}}{1+\bar{e}\cos \bar{v}} + \frac{\bar{e}\cos \bar{v}}{1+(1-\bar{e}^2)^{\frac{1}{2}}} \right] \right\} \quad (\text{III.12})$$

$$\delta \dot{r}_s = -\alpha_1 \left\{ 2\sin^2 \bar{I} (1+\bar{e}\cos \bar{v})^2 \sin 2\bar{u} + (1-3\cos^2 \bar{I}) \bar{e} \sin \bar{v} \left[-\frac{(1-\bar{e}^2)^{\frac{1}{2}}}{2} + \frac{(1+\bar{e}\cos \bar{v})^2}{1+(1-\bar{e}^2)^{\frac{1}{2}}} \right] \right\} \quad (\text{III.13})$$

$$\delta r \dot{v}_s = \alpha_1 \left\{ \sin^2 \bar{I} \left[2\cos 2\bar{u} + 2\bar{e}\cos(2\bar{u}-\bar{v}) + \bar{e}\cos \bar{v} \cos 2\bar{u} \right] (1+\bar{e}\cos \bar{v}) - (1+\bar{e}\cos \bar{v})(1-3\cos^2 \bar{I}) \left[\frac{3}{2} + \bar{e}\cos \bar{v} \frac{2+(1-\bar{e}^2)^{\frac{1}{2}}}{1+(1-\bar{e}^2)^{\frac{1}{2}}} + \frac{\bar{e}^2-2(\bar{e}\sin \bar{v})^2}{2[1+(1-\bar{e}^2)^{\frac{1}{2}}]} \right] \right\} \quad (\text{III.14})$$

$$\delta \dot{I}_s = \alpha \sin \bar{I} \cos \bar{I} \left\{ 3 \left[\cos 2\bar{u} + \bar{e}\cos(2\bar{u}-\bar{v}) + \bar{e}\cos(2\bar{u}+\bar{v}) \right] \right\} \quad (\text{III.15})$$

$$\delta \Omega_s = -\alpha \cos \bar{I} \left\{ 6(\bar{v}-\bar{M} + \bar{e}\sin \bar{v}) - 3 \left[\sin 2\bar{u} + \bar{e}\sin(2\bar{u}-\bar{v}) - \bar{e}\sin(2\bar{u}+\bar{v}) \right] \right\} \quad (\text{III.16})$$

$$\begin{aligned}
\delta u_s = -\frac{\alpha}{2} \left\{ & 6(1-5\cos^2 \bar{I}) (\bar{v}-\bar{M}) \right. \\
& +4 \left[1-6\cos^2 \bar{I} + \frac{1-3\cos^2 \bar{I}}{1+(1-\bar{e}^2)^{\frac{1}{2}}} \right] \bar{e} \sin \bar{v} \\
& + (1-3\cos^2 \bar{I}) \frac{2(\bar{e} \sin \bar{v})(\bar{e} \cos \bar{v})}{1+(1-\bar{e}^2)^{\frac{1}{2}}} \\
& + 2(5\cos^2 \bar{I}-2) \bar{e} \sin (2\bar{u}-\bar{v}) \\
& \left. + (7\cos^2 \bar{I}-1) \sin 2\bar{u} + 2\cos^2 \bar{I} \bar{e} \sin (2\bar{u}-\bar{v}) \right\} \quad (\text{III.17})
\end{aligned}$$

where

$$\alpha = \frac{J_2 a^2}{4p^2}$$

$$\alpha_1 = \alpha \left[\frac{\mu_e}{\bar{p}} \right]^{\frac{1}{2}}$$

The difference between the true and mean anomalies needed to compute $\delta \Omega_s$ and δu_s is given by:

$$(\bar{v}-\bar{M}) = (\bar{v}-\bar{E}) + (\bar{E}-\bar{M})$$

where \bar{E} is the eccentric anomaly and (Ref. 8):

$$(\bar{v}-\bar{E}) = \sin^{-1} \left[\left(\frac{\bar{e} \sin \bar{v}}{1+\bar{e} \cos \bar{v}} \right) \left(\frac{(1-\bar{e}^2)^{\frac{1}{2}} + 1 + \bar{e} \cos \bar{v}}{1+(1-\bar{e}^2)^{\frac{1}{2}}} \right) \right]$$

and

$$(\bar{E}-\bar{M}) = \frac{(1-\bar{e}^2)^{\frac{1}{2}} \bar{e} \sin \bar{v}}{1+\bar{e} \cos \bar{v}}$$

These short period variations (specifically δr_s , $\delta \dot{r}_s$ and $\delta r \dot{v}_s$) include the effect of Kozai's perturbed semi-major axis (Ref. 1) as given previously in Section III.2. This additional variation does not have to be accounted for separately.

Appendix V gives the FORTRAN coding for the Frazer algorithm (includes long period variations) and Figures 14 through 20 show theoretical results obtained in the Keplerian elements by applying the short period portion as described above. The example used is the same as that previously given for the Kozai method in Tables II and III. The mean longitude variations, δL_s , given in Figure 20 are defined by:

$$\delta L_s = \delta \omega_s + \delta M_s$$

The figures show quasi-mean (short period variations removed) and classical Keplerian elements for one orbital revolution of a satellite. Secular variations were removed for ease of plotting.

If the computations of these variations are restricted to near-circular orbits, the above equations (with $\bar{e}=0$) reduce to:

$$\delta r_s = \alpha \bar{p} \sin^2 \bar{i} \cos 2\bar{u}$$

$$\delta \dot{r}_s = -2\alpha_1 \sin^2 \bar{i} \sin 2\bar{u}$$

$$\delta r \dot{v}_s = \alpha_1 \left[2 \sin^2 \bar{i} \cos 2\bar{u} - \frac{3}{2} (1 - 3 \cos^2 \bar{i}) \right]$$

$$\delta i_s = 3\alpha \sin \bar{i} \cos \bar{i} \cos 2\bar{u}$$

$$\delta \Omega_s = 3\alpha \cos \bar{i} \sin 2\bar{u}$$

$$\delta u_s = -\frac{\alpha}{2} (7 \cos^2 \bar{i} - 1) \sin 2\bar{u}$$

These approximate equations yield short period variations with errors varying as a function of the eccentricity. Table V shows some typical errors, encountered at various eccentricities, caused by using the approximate rather than the full equations. Since these are just isolated examples, they must not by any means be considered as maximum errors which could be obtained. The errors given are the differences between elements obtained after applying the equations III.12-17 and the approximate equations above to an input vector.

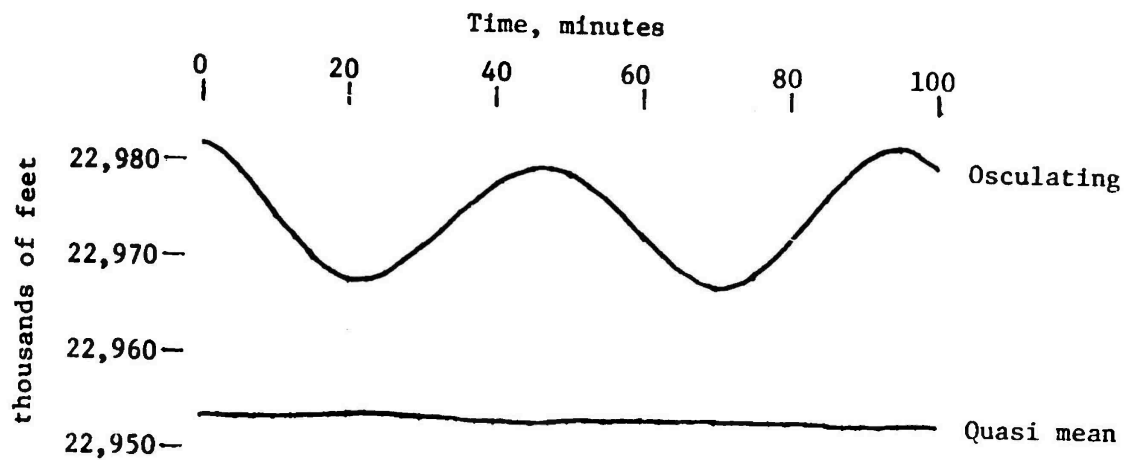


Figure 14. Frazer Semi-Major Axis Short Period Variations

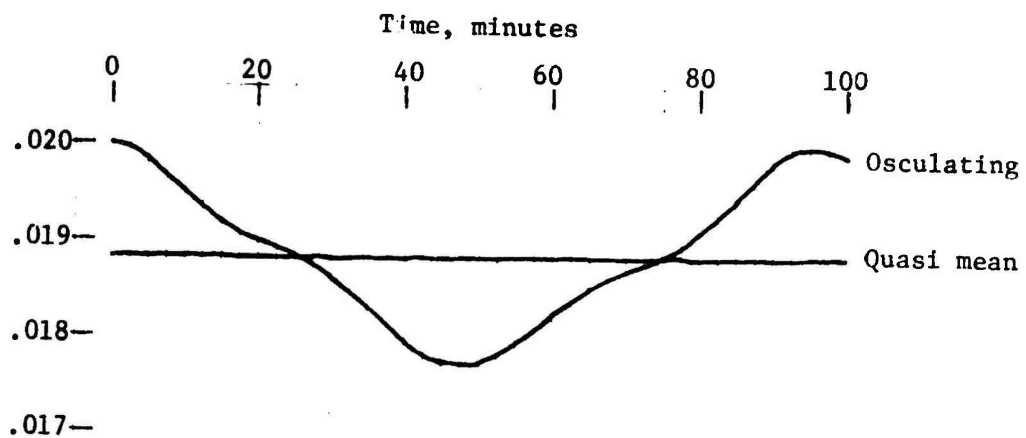


Figure 15. Frazer Eccentricity Short Period Variations

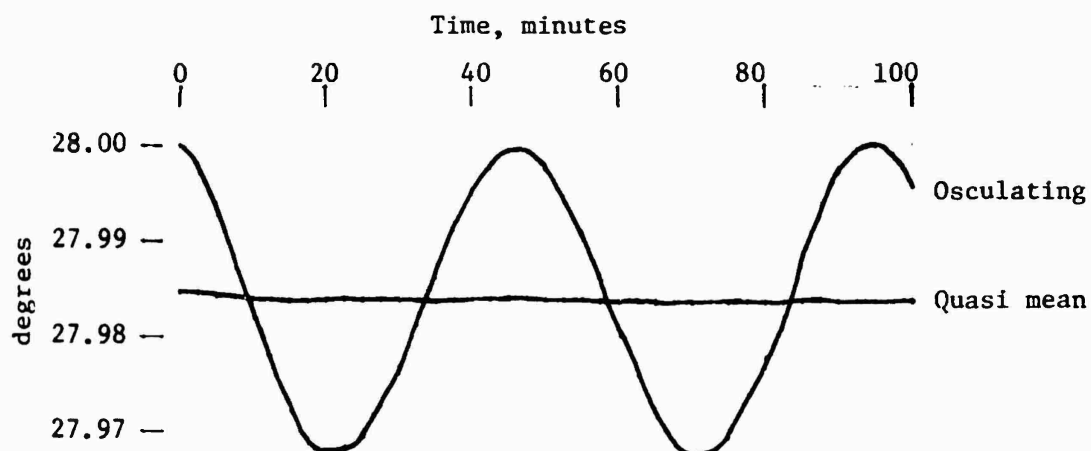


Figure 16. Frazer Inclination Short Period Variations

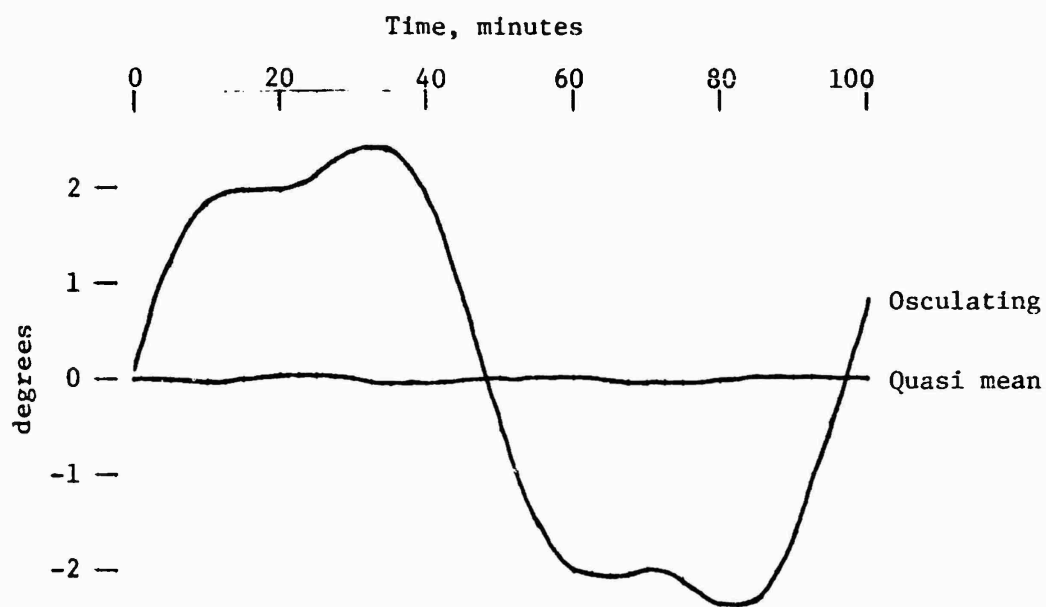


Figure 17. Frazer Argument of Perigee Short Period Variations

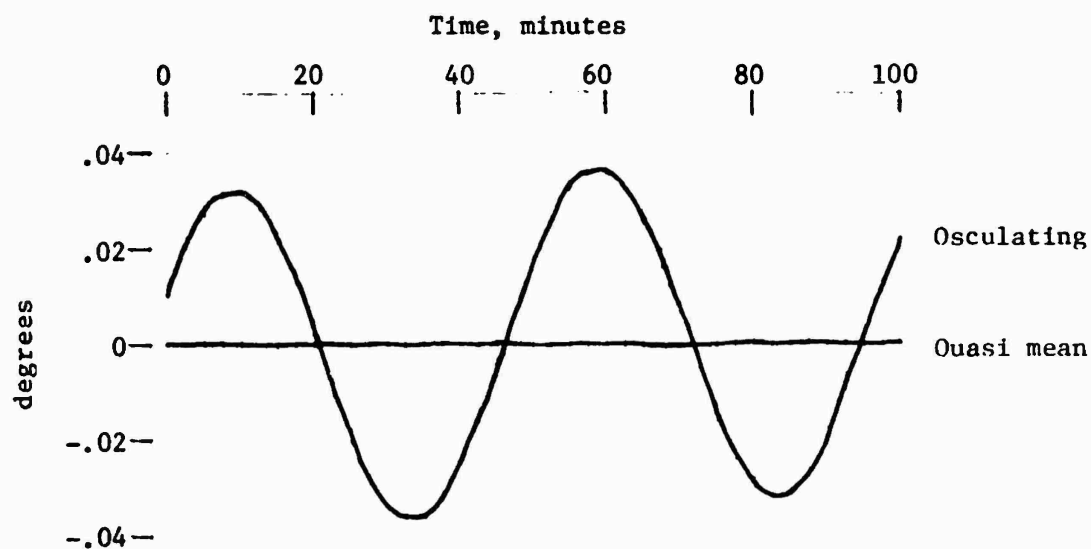


Figure 18. Frazer Right Ascension of Ascending Node Short Period Variations

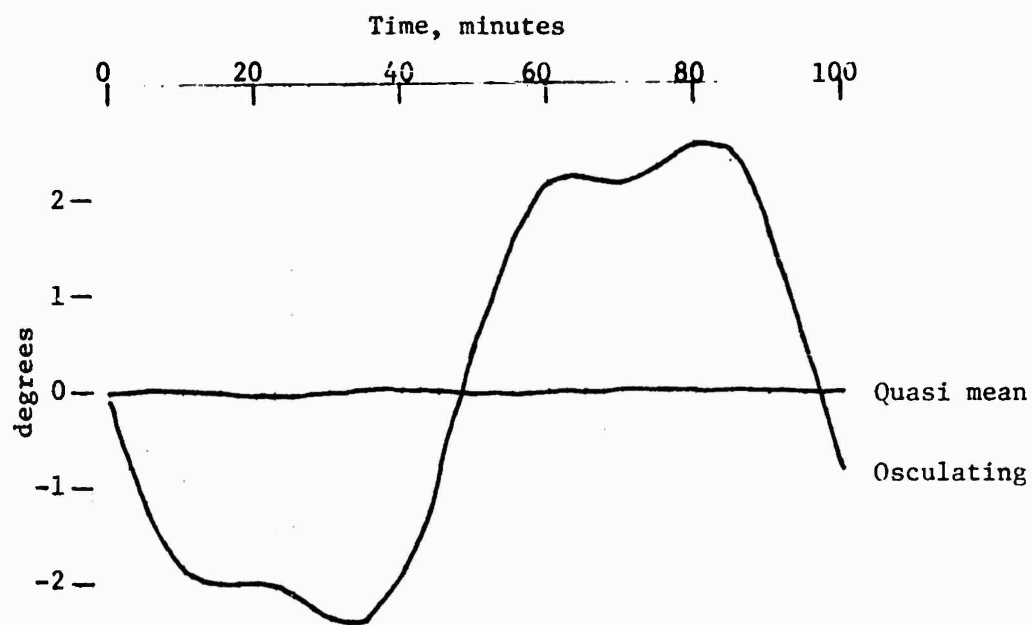


Figure 19. Frazer Mean Anomaly Short Period Variations

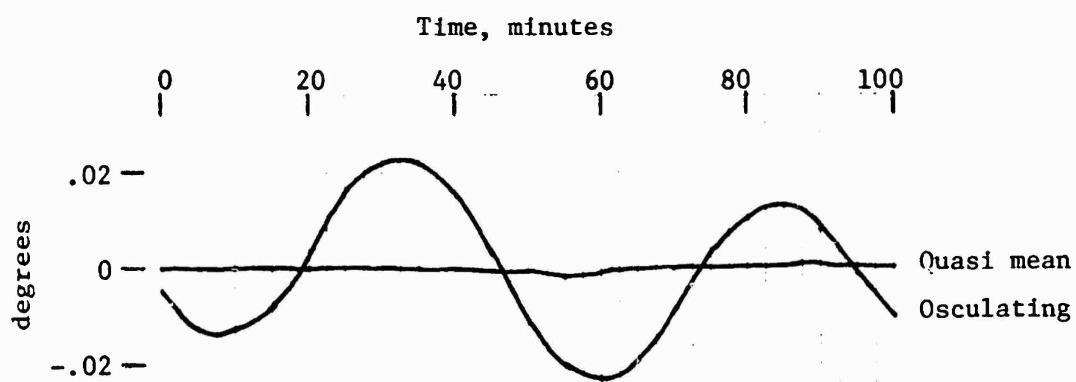


Figure 20. Frazer Mean Longitude Short Period Variations

TABLE V

Examples of Errors Caused by Using
Approximate Short Period Variations

	Eccentricity		
	0.02	0.125	0.6
δr (ft.)	98.	385.	3383.
$\delta \dot{r}$ (ft./sec.)	0.05	1.29	0.75
$\delta r \dot{v}$ (ft./sec.)	0.26	0.42	5.42
δi (deg.)	0.0002	0.0002	0.0006
$\delta \Omega$ (deg.)	0.0030	0.0073	0.0064
δu (deg.)	0.0053	0.0392	0.0206
δx (ft.)	628.	3189.	3612.
δy (ft.)	633.	577.	5675.
δz (ft.)	725.	1090.	788.
$\delta \dot{x}$ (ft./sec.)	0.04	2.20	3.46
$\delta \dot{y}$ (ft./sec.)	1.12	3.72	10.33
$\delta \dot{z}$ (ft./sec.)	0.62	1.85	2.97
δa (ft.)	257.	181.	28717.
δe	0.000006	0.000023	0.000261
$\delta \omega$ (deg.)	0.0482	0.0280	0.0352
δM (deg.)	0.0426	0.0181	0.0084

III.4 Inverse Computations

In both the Kozai and Frazer forms of the variation equations, the variations are computed as functions of the mean elements. If it is desired to transform osculating to mean elements the equations cannot be used directly. Instead, they are used in an iterative sense as described below.

First an approximate set of mean elements is obtained (usually the osculating elements). These are used to compute variations and approximate osculating elements are obtained and compared to the known osculating elements. The differences between the two sets are the errors in the computed osculating elements caused by errors in the approximate mean elements. These mean elements are then corrected by the amounts of the differences concluding the first iteration. This process is repeated until some convergence criteria are satisfied.

When using the Frazer method and convergence criteria of 1.0 feet and 0.001 ft/sec, convergence is almost always achieved in three iterations. When using the Kozai method, convergence is sometimes difficult to achieve for near-circular orbits. After forty iterations, significant errors may still be present in argument of perigee and mean anomaly. However, a method involving matrix inversion (Ref. 9) can be used to yield quick solutions for the Kozai method.

Appendix VI shows the FORTRAN coding which performs the iteration control when going from osculating to mean elements with the Frazer method. Table VI shows the results of using the iterative technique to compute mean from osculating elements using the Frazer method. Although in the example shown, the long period variations are larger than the short period in the Cartesian elements, the reverse is true in the Keplerian elements. Also, the long period variations in the Cartesian elements make no significant contribution toward variation in the semi-major axis.

TABLE VI
EXAMPLE OF FRAZER INVERSE COMPUTATIONS

INITIAL OSCULATING VECTORS		a	e	i	ω	Ω	M
		22974394.	.019253	27.984616	16.819571	108.579818	301.112438
		x	y	z	\dot{x}	\dot{y}	\dot{z}
		8008296.	19964142.	..7413602.	-20727.6632	11024.1029	8573.4654
FIRST ITERATION							
VARIATIONS							
SHORT PERIOD		3068.	-194.	2968.	-5.9700	9.6882	6.5530
LONG PERIOD		14777.	-481	-7568.	9.0979	3.5841	-5.5920
TOTAL		17846.	-676.	-4600.	3.1276	13.2723	0.9610
NEW ESTIMATED MEAN VECTOR		7990451.	19964818.	-7409002.	-20730.7911	11010.8306	8572.5043
SECOND ITERATION							
VARIATIONS							
SHORT PERIOD		3064.	-179.	2978.	-5.9864	9.6802	6.5733
LONG PERIOD		14789.	-473.	-7561	9.1044	3.5972	-5.5923
TOTAL		17852.	-652.	-4583.	3.1180	13.2774	0.9810
OSCULATING ERRORS		-6.	-23.	-17.	0.0099	-0.0052	-0.0200
NEW ESTIMATED MEAN VECTOR		7990445.	19964794.	-7409019.	-20730.7812	11010.8255	8572.4844
THIRD ITERATION							
VARIATIONS							
SHORT PERIOD		3063.	-179.	2978.	-5.9864	9.6802	6.5733
LONG PERIOD		14789.	-473.	-7561.	9.1044	3.5972	-5.5923
TOTAL		17852.	-652.	-4583.	3.1180	13.2774	0.9810
OSCULATING ERRORS		-0.04	-0.04	-0.04	-0.00002	-0.00002	0.00005
MEAN KEPLERIAN VECTOR		22952977.	0.018754	27.984143	18.085366	108.609094	299.836032
		\bar{a}	\bar{e}	\bar{i}	$\bar{\omega}$	$\bar{\Omega}$	\bar{M}

SECTION IV

APPLICATIONS

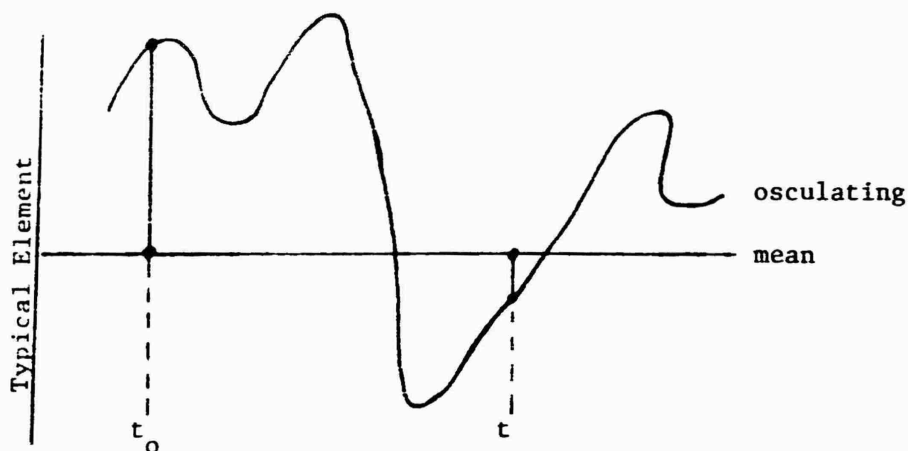
IV.1 Introduction

The preceding sections have presented the mathematical expressions describing variations in the orbital elements and have shown numerical examples obtained from the applications of those expressions. The purpose of this section is to show how knowledge of these variations can be used to advantage in orbital support. At the AFETR RTCS, two major uses of these variations have been exploited. These two uses are described below.

IV.2 Trajectory Generation

The major use to which element variations have been applied at the RTCS is that pertaining to trajectory generation. This is based upon the premise that, given elements at epoch, elements at any time can be obtained if the element variations can be computed. This can be easily accomplished using the mathematical expressions given in the preceding sections.

For example, suppose that the position and velocity of an object is given in the osculating geocentric inertial Cartesian system at epoch and the position and velocity is desired in the same system at some other time. One way to accomplish this trajectory generation would be by numerical integration of the equations of motion where accelerations in the Cartesian system are computed based on models of the earth's gravity and atmosphere. But such a trajectory generation can be accomplished through element variations, also. Such a generation using the methods presented in the preceding sections would require a four-step process. First, mean elements would be obtained from the osculating (periodic variations removed) using inverse computations (Section III.4). Second, element rates (secular variations) would be computed (Section II). Third, these rates would be applied to the mean elements at epoch to obtain the mean elements at the time of interest. Fourth, the mean elements at the time of interest are converted to osculating (periodic variations added) thus completing the trajectory generation. This procedure is shown pictorially by:



Mathematical expressions for accomplishing the first, second and fourth parts above have been presented. The third part, comprising the update of the mean elements from epoch, t_0 , to time of interest, t , is described below. Often, the mean elements and their rates at epoch are given in the form of an Air Force Space Defense Center 5-card element set (SDC bulletin). Information contained on this bulletin includes the following mean elements and their time derivations at epoch (see Appendix I):

- \bar{a}_0 = mean semi-major axis
- $\dot{\bar{a}}$ = derivative of \bar{a}
- $\frac{\dot{\bar{a}}}{2}$ = half of derivative of \bar{a}
- \bar{e} = mean eccentricity
- $\dot{\bar{e}}$ = derivative of \bar{e}
- $\frac{\dot{\bar{e}}}{2}$ = half of derivative of \bar{e}
- \bar{i}_0 = mean inclination
- $\dot{\bar{i}}$ = derivative of \bar{i}
- $\bar{\omega}_0$ = mean argument of perigee
- $\dot{\bar{\omega}}$ = derivative of $\bar{\omega}$
- $\frac{\dot{\bar{\omega}}}{2}$ = half of derivative of $\bar{\omega}$
- $\bar{\Omega}_0$ = mean right ascension of ascending node
- $\dot{\bar{\Omega}}$ = derivative of $\bar{\Omega}$
- $\frac{\dot{\bar{\Omega}}}{2}$ = half of derivative of $\bar{\Omega}$
- \bar{M}_0 = mean mean anomaly
- \bar{n} = mean mean motion (derivative of \bar{M})
- $\frac{\dot{\bar{n}}}{2}$ = half of derivative of \bar{n}

$\frac{\ddot{n}}{6}$ = sixth of derivative of \dot{n}

$\frac{\ddot{n}}{24}$ = twenty fourth of derivative of \ddot{n}

As can be seen, these bulletin parameters are nothing more than the coefficients of a MacLaurin's series expansion about epoch. The mean element update can then be accomplished by:

$$\Delta t = t - t_0$$

$$\bar{a} = \bar{a}_0 + \dot{a}\Delta t + \frac{\ddot{a}}{2}\Delta t^2 \quad (\text{IV.1})$$

$$\bar{e} = \bar{e}_0 + \dot{e}\Delta t + \frac{\ddot{e}}{2}\Delta t^2 \quad (\text{IV.2})$$

$$\bar{i} = \bar{i}_0 + \dot{i}\Delta t \quad (\text{IV.3})$$

$$\bar{\omega} = \bar{\omega}_0 + \dot{\omega}\Delta t + \frac{\ddot{\omega}}{2}\Delta t^2 \quad (\text{IV.4})$$

$$\bar{\Omega} = \bar{\Omega}_0 + \dot{\Omega}\Delta t + \frac{\ddot{\Omega}}{2}\Delta t^2 \quad (\text{IV.5})$$

$$\bar{M} = \bar{M}_0 + \bar{n}\Delta t + \frac{\dot{n}}{2}\Delta t^2 + \frac{\ddot{n}}{6}\Delta t^3 + \frac{\ddot{n}}{24}\Delta t^4 \quad (\text{IV.6})$$

In practice \dot{i} and $\frac{\ddot{n}}{24}$ are usually zero.

The above method for updating mean eccentricity can sometimes cause problems. The secular variation in eccentricity for most objects is caused principally by atmospheric drag which has the effect of circularizing the orbits. In other words \dot{e} and \ddot{e} are usually both negative. When \bar{e}_0 is small, \bar{e} can be negative for some values of Δt . This creates problems when trying to transform these mean elements into osculating Cartesian elements. This problem can be circumvented if it is assumed that the eccentricity decay is due to a decrease in apogee height and that perigee height remains constant. This is usually a valid assumption, especially if the element rates were computed based on equations derived from that assumption (Section II). Then:

$$\bar{e} = 1 - \frac{\bar{a}_0 (1 - \bar{e}_0)}{\bar{a}} \quad (\text{IV.7})$$

This method of trajectory generation has a major advantage over numerical integration. Since it is not a step-by-step procedure, the vector at time of interest can be immediately computed with no regard for vectors at intermediate times. When Δt is large, this advantage results in a considerable savings in computation time. Being a step-by-step procedure, numerical integration is subject to round-off and truncation errors which can be fatal when Δt is large.

The mean element update method of trajectory generation has proved to be sufficiently accurate for satellite acquisition at AFETR Mipir radar sites. The FORTRAN coding for this procedure is given in Appendix VII. This technique was compared against numerical integration for two cases: with and without drag. Table VII shows the initial conditions used for both methods. The resulting orbital characteristics are also shown as well as the ballistic coefficient used with the U. S. Standard Atmosphere 1962 model for drag computation. The gravity model used with the numerical integration is given in Table III. The central gravity term, μ_e , and the zonal coefficients, J_2 and J_3 were also used for the mean element computations.

The mean elements and their rates at epoch, obtained from the initial conditions as shown in Section II, are given in Table VIII. The differences between the trajectories are presented in intrack, crosstrack and radial components in Tables IX and X. Differences are shown at ten minute intervals for the first revolution, the last revolution of the first day and the last revolution of the week. The differences obtained in these examples are due to the use of tesseral harmonics in the integrated trajectory and to inadequacies inherent in the mean elements trajectory generation scheme. The differences are obtained by subtracting the mean element updated trajectory points from the numerically integrated trajectory. Note that in both the vacuum and drag cases, the radial and crosstrack errors oscillate about zero with ever increasing amplitude and very little secular variation, while the intrack oscillates about an ever-growing mean value.

Drag trajectory generations were also performed with zero values for $\frac{a}{2}$, $\frac{e}{7}$, $\frac{u}{7}$, and $\frac{n}{6}$. The resulting trajectory errors in radial and intrack components were considerably smaller than those shown in Table X. For example, mean differences at the end of one week were:

radial = -2226 ft
crosstrack = 2179 ft
intrack = -131289 ft

For some reason, these terms adversely affect the accuracy of this drag trajectory generation. It could be that they are useful for objects with high ballistic coefficients or in extremely low orbits. However, all cases studied have shown that optimum results are obtained with the above mentioned parameters set to zero.

TABLE VII
THEORETICAL TRAJECTORY INITIAL CONDITIONS

$x = 17837622. \text{ ft.}$
 $y = 11170525. \text{ ft.}$
 $z = 4559553. \text{ ft.}$
 $\dot{x} = -14197. \text{ ft./sec.}$
 $\dot{y} = 17945. \text{ ft./sec.}$
 $\dot{z} = 11635. \text{ ft./sec.}$

Trajectory Characteristics:

$h_p = 100 \text{ nm}$
 $h_a = 150 \text{ nm}$
 $P = 89 \text{ min.}$

Ballistic Coefficient:

$$B = \frac{C_D A}{W} = 0.01 \text{ ft}^2/\text{lb}$$

TABLE VIII
THEORETICAL MEAN ELEMENTS AND RATES

	\bar{a}	= 1.03625778 earth radii (ER)
	\bar{e}	= .006798
	\bar{i}	= 29.999538 deg
	$\bar{\omega}$	= 16.219243 deg
	$\bar{\Omega}$	= 9.998874 deg
	\bar{M}	= 8.781831
*	\dot{a}	= -2.843243×10^{-4} ER/day
*	$\frac{\ddot{a}}{2}$	= -4.020530×10^{-6}
*	\dot{e}	= -2.725106×10^{-4}
*	$\frac{\ddot{e}}{2}$	= -3.853477×10^{-6}
	$\dot{\omega}$	= 12.086671 deg/day
*	$\frac{\ddot{\omega}}{2}$	= 5.758724×10^{-3}
	$\dot{\Omega}$	= -7.612567 deg/day
*	$\frac{\ddot{\Omega}}{2}$	= -0.003627 deg/day ²
	\bar{n}	= 16.14925696 revs/day
*	$\frac{\dot{n}}{2}$	= 0.00332323 revs/day ²
*	$\frac{\ddot{n}}{6}$	= 3.208824×10^{-5}

*These rates set to zero for vacuum trajectory

TABLE IX
VACUUM TRAJECTORY DIFFERENCES

Prediction Time (min)	Prediction Errors (ft)		
	Radial	Crosstrack	Intrack
0	0.	0.	0.
10	16.	16.	- 32.
20	- 3.	32.	-104.
30	25.	67.	-217.
40	78.	97.	-299.
50	108.	22.	-406.
60	99.	- 26.	-512.
70	- 4.	93.	-625.
80	- 63.	201.	-542.
(1 rev) 90	-230.	193.	-228.
1350	174.	- 75.	4418.
1360	116.	1829.	4122.
1370	55.	2870.	4012.
1380	- 52.	2470.	4048.
1390	-122.	926.	4185.
1400	-150.	- 890.	4356.
1410	- 77.	- 2253.	4532.
1420	- 52.	- 2612.	4719.
1430	- 53.	- 1677.	4807.
(1 day) 1440	- 32.	108.	4847.
9990	-290	10113.	34607.
10000	89.	18084.	34722.
10010	426.	17421.	34394.
10020	561.	8470.	33737.
10030	448.	- 4440.	33057.
10040	68.	-15140.	32590.
10050	-322.	-18589.	32601.
10060	-666.	-13065.	33235.
10070	-765.	- 1106.	34174.
(1 week) 10080	-477.	11436.	35046.
Last rev mean	- 93.	1318.	33816.

TABLE X
DRAG TRAJECTORY DIFFERENCES
(POLYNOMIAL UPDATE)

Prediction Time (min)	Prediction Errors (ft)		
	Radial	Crosstrack	Intrack
0	0.	0.	0.
10	24.	16.	- 3.
20	34.	32.	- 41.
30	112.	67.	- 172.
40	208.	97.	- 367.
50	238.	22.	- 664.
60	162.	- 27.	- 951.
70	- 38.	91.	- 1111.
80	- 208.	201.	- 927.
(1 rev) 90	- 391.	194.	- 373.
1350	- 941.	22.	- 29273.
1360	1126.	1886.	- 29395.
1370	2972.	2854.	- 32253.
1380	3668.	2385.	- 36866.
1390	2904.	817.	- 41387.
1400	968.	- 967.	- 43973.
1410	- 1193.	- 2266.	- 43544.
1420	- 2639.	- 2556.	- 40406.
1430	- 2612.	- 1574.	- 36347.
(1 day) 1440	- 1066.	209.	- 33547.
9990	-72055.	19431.	-1654791.
10000	-53853.	14706.	-1659008.
10010	-41571.	2075.	-1685803.
10020	-39677.	-10114.	-1723967.
10030	-50072.	-18215.	-1756987.
10040	-67623.	-17533.	-1769944.
10050	-84648.	- 8300.	-1757641.
10060	-92839.	5071.	-1727493.
10070	-87841.	16024.	-1695574.
(1 week) 10080	-72103.	19268.	-1678511.
Last rev mean	-66228.	2241.	-1710972.

The differences shown above resulting from the use of analytical secular variations are considerably larger than those obtained from numerical computations using real data (Section IV.3, Table XIV).

There is good agreement between numerical and mean element trajectories for the vacuum case (Table IX). Therefore the large intrack differences obtained for the drag case must be due to either drag-affected secular rates or their application to the trajectory generation problem. If a logarithmic rather than polynomial update scheme is used the intrack differences are considerably decreased. The logarithmic scheme is based upon the fact that the mean motion is a logarithmic function of time:

$$\bar{n} = \bar{n}_0 + \log_e (1 + 2 \frac{\dot{n}}{2} \Delta t)$$

and the mean semi-major axis is given by:

$$\bar{a} = \bar{a}_0 \left[\frac{\bar{n}_0}{\bar{n}} \right]^{\frac{2}{3}}$$

The mean mean anomaly can then be updated by:

$$\bar{M} = \bar{M}_0 + \bar{n}_a \Delta t$$

where

$$\bar{n}_a = \bar{n}_0 + \Delta n$$

and

$$\Delta n = \int_0^{\Delta t} \log_e (1 + \frac{\dot{n}}{2} t) dt$$

which, after changing limits and applying a four-point Gauss' method of approximate quadratures, becomes (Ref. 10):

$$\Delta n = \sum_{i=1}^4 A_i \log_e \left[1 + \frac{\dot{n}}{2} \Delta t X_i \right]$$

where A_i and X_i are quadrature values:

i	A_i	X_i
1	0.34785485	0.93056815
2	0.65214515	0.66999052
3	0.65214515	0.33000947
4	0.34785485	0.06943184

Using this logarithmic scheme of mean mean anomaly update, the differences shown in Table XI were obtained. As can be seen, the intrack differences are much improved over those given above which suggests that this method should be extensively studied both experimentally and analytically. However, preliminary results indicate that the improvement shown is typical of what can be achieved.

TABLE XI
DRAG TRAJECTORY DIFFERENCES
(LOGARITHMIC UPDATE)

Prediction Time (min)	Prediction Errors (ft)		
	Radial	Crosstrack	Intrack
0	0.	0.	0.
10	24.	16.	- 3.
20	34.	32.	- 41.
30	112.	67.	- 172.
40	208.	97.	- 367.
50	238.	22.	- 664.
60	162.	- 27.	- 951.
70	- 38.	91.	- 1111.
80	- 208.	201.	- 926.
(1 rev) 90	- 391.	194.	- 373.
1350	- 959.	22.	-23497.
1360	1045.	1885.	-23532.
1370	2824.	2852.	- 26214.
1380	3479.	2384.	-30588.
1390	2722.	816.	-34860.
1400	838.	- 966.	-37246.
1410	- 1250.	- 2265.	-36704.
1420	- 2638.	- 2554.	-33539.
1430	- 2596.	- 1572.	-29494.
(1 day) 1440	- 1088.	209.	-26677.
9990	- 6191.	18850.	61152.
10000	7573.	14260.	58903.
10010	16150.	1992.	39836.
10020	16693.	- 9791.	14265.
10030	7703.	-17655.	- 5041.
10040	- 6151.	-17014.	- 7541.
10050	-18414.	- 8062.	9340.
10060	-22944.	4920.	38732.
10070	-17505.	15544.	67476.
(1 week) 10080	- 4795.	18673.	82652.
Last rev mean	- 2788.	2172.	35977.

IV.3 Orbit Determination

Another use to which element variations have been applied at the RTCS is that pertaining to orbit determination. This technique has been put to full use in the CDC 3100 computer program, CASS (Ref 10).

Orbit determination using mean elements is accomplished as follows. First, each pass of tracking data is reduced to a vector (position and velocity) using some method of orbit determination. Second, all such vectors are transformed to mean Keplerian elements using the inverse computations described in Section III.4. Third, polynomials in time are passed in a least squares sense through like elements, one from each pass. The polynomial coefficients thus determined are identical in definition to the parameters of an SDC bulletin (Appendix I). These coefficients then represent the multi-pass solution and can be used to predict future positions of the object as shown in Section IV.2.

In CASS, however, the polynomial coefficients are not the ones appearing on the final transmitted bulletin. It is necessary to analytically recompute some of the parameters in order to preserve known relationships among them (e.g. \dot{a} and \dot{e}). Some of these relationships are given in Section II. Examples of actual single-pass mean elements used and the polynomial and analytical bulletins thus obtained are given in Tables XII, XIII and XIV. Prediction errors for the analytical bulletin are given in Table XV in radial, crosstrack and intrack components. The solution and prediction errors were obtained using actual tracking data from AFETR Mipir radars. These errors are caused by several factors. First, the mean elements and their rates at epoch contain errors due to their computations being based on imperfect tracking data. Second, the vectors against which the predictions are compared to produce residuals are based on imperfect tracking data and contain errors. Third, the actual forces influencing the object are not completely modeled in the mean elements updating scheme. Examples of some not included in the computations are higher order gravity terms and atmospheric density variations. Approximately 20.7 days after epoch (17 August 1970) a large geomagnetic disturbance occurred which significantly effected the prediction errors (Table XV).

Notice in Table XIII that the single-pass mean element residuals from the polynomial solution show periodic errors in mean longitude despite the modeling of periodic variations in CASS. The cause of the residual long period variation is not known. It may be that they are due to unmodeled gravity or drag forces.

TABLE XII

CASS SINGLE-PASS MEAN ELEMENTS FOR ORBIT DETERMINATION

~~MEAN ELEMENTS SUMMARY FOR 06J 1060~~

DAY	TIME	MA	ME	MI	MAP	MRAN	MMA	STATION
100	062503	1.09330797	.014695	31.760553	346.935052	322.738834	129.229110	91A
100	062527	1.09254407	.014697	31.768397	61.298528	273.185968	75.287771	00A
100	062557	1.09307924	.014868	31.774014	137.103627	224.875233	41.334355	12A
200	062558	1.09301584	.014798	31.747059	186.730218	186.887108	125.440879	12A
200	062638	1.09299031	.014606	31.751766	253.264572	149.353777	88.044432	12A

TABLE XIII

CASS POLYNOMIAL MEAN ELEMENT RESIDUALS

MA	ME	MF	MAP	MRAN	MAP+MRA
-0.000003	.0000001	.0001948	.0589090	.00000843	.0237936
-0.000004914**	-0.0002124**	.0020352	-1.6744449**	-0.0170202**	-0.0655079
.0000026	-0.0000008	.0136562	-0.0781195	.0006999	.0259819
-0.0000038	.0000012	-0.0112967	-0.1177944	-0.0010272	-0.352510
.0000015	-0.0000005	-0.0000006	.1369923	.0004199	-0.0284012

** Point edited from solution

TABLE XIV

CASS POLYNOMIAL AND ANALYTICAL ORBIT SOLUTIONS

Element	Derivatives		
	Value	First	Second
Polynomial			
SEMI-MAJOR AXIS	1.092998677E 00	-6.44654047E-06	-2.06021578E-07
ECCENTRICITY	1.46959952E-02	-1.97389699E-05	-4.52330954E-07
INCLINATION	3.17603579E 01	0	0
ARGUMENT OF PERIGEE	2.53127577E 02	9.54468554E 00	0
RIGHT ASCENSION OF ASCENDING NODE	1.49353359E 02	-6.21794185E 00	-8.41913575E-05
LONG ANOMALY	8.82081332E 01	1.49092993E 01	1.63795410E-05
Analytical			
SEMI-MAJOR AXIS	1.092998652E 00	-1.60104093E-06	-3.24272707E-11
ECCENTRICITY	1.46959952E-02	-1.44328835E-06	-2.92321710E-11
INCLINATION	3.17603579E 01	0	0
ARGUMENT OF PERIGEE	2.53127577E 02	9.54004701E 00	0
RIGHT ASCENSION OF ASCENDING NODE	1.49353359E 02	-6.21794185E 00	-8.41913575E-05
LONG ANOMALY	8.82081332E 01	1.49093121E 01	1.63795410E-05

TABLE XV

CASS ANALYTICAL BULLETIN PREDICTION ERRORS

<u>Time From Epoch (days)</u>	<u>Prediction Errors (ft)</u>		
	<u>Radial</u>	<u>Crosstrack</u>	<u>Y track</u>
3.2	- 3.	747.	- 4656.
4.2	466.	- 2778.	- 5892.
8.1	-3206.	3673.	8994.
9.0	-4083.	3768.	9482.
15.1	-4344.	2393.	8799.
17.1	-3757.	775.	9588.
21.2	-1490.	-13790.	25658.
22.1	-4807.	- 8062.	24480.
22.2	-4287.	-14080.	31676.
24.1	-3066.	- 2328.	51068.
25.0	-1906.	2045.	67755.
28.0	-2452.	- 9273.	144416.

Comparisons between SDC bulletin parameters and computed secular variations were presented in Section II, Table I. Here note the differences between the polynomial coefficients and the analytical parameters in Table XIV.. Those parameters analytically recomputed were: \bar{a} , \dot{a} , $\frac{\dot{a}}{Z}$, \dot{e} , $\frac{\dot{e}}{Z}$, ω , and n using methods similar to those given in Section II (Ref 11).

APPENDIX I

SPACE DEFENSE CENTER 5-CARD BULLETIN

(((((
1 04483 U 00028 70 057 B 0 03.3 001320 0307 0 1
2 04483 40893.85496469 233.5949 247.0671 129.4386 .0327040 048.3932 6
3 04483 15.53805068 .012682872 -5.34388 4.84710 -10527-2 0 4
4 04483 00000000-0 -98094-2 88975-2 28643-6 8
5 04483 01.06351376 -1157451-2 1574609-5 2
)))))

(Key on following page)

APPENDIX II
SUBROUTINE DTPDA

(Semi-Major Axis Decay Rate Computation - See SECTION II)


```

SUBROUTINE DTPDAT(FMU,AF,E2,A,E,FI,FO,RCOEFF,ADOT)
C
C THE PURPOSE OF THIS ROUTINE IS TO COMPUTE DRAG DECAY
C RATES OF APOGEE, PERIGEE AND SEMI-MAJOR AXIS BY
C INTEGRATION USING SIMPSONS RULE.
C
C INPUTS ARE
C FMU=EARTH GRAVITY CONSTANT(FT**3/SEC**2)
C AF=EARTH SEMI-MAJOR AXIS(FT)
C E2=EARTH ECCENTRICITY SQUARED
C A=ORBIT SEMI-MAJOR AXIS(FT)
C E=ORBIT ECCENTRICITY
C FI=ORBIT INCLINATION(RAD)
C FO=ORBIT ARGUMENT OF PERIGEE(RAD)
C BCOEFF=OBJECT BALLISTIC COEFFICIENT (CD*A/W) (FT**2/LB)
C WHERE A=REFERENCE AREA
C CD=COEFFICIENT OF DRAG
C W=OBJECT WEIGHT
C
C OUTPUT IS
C ADOT=DECAY RATE OF ORBIT SEMI-MAJOR AXIS(FT/DAY)
C
C ATMOSPHERE MODEL SUBROUTINE IS ATMOS
C
C DATA(PI=3.1415926535)
C
C TPI = 2. * PI
C SDTP=-36400.*SQRT(A*FMU)/TPI
C FE=E2/(1.-E2)
C D=A*(1.-E*E)
C SO=SINF(FO)
C CO=COSF(FO)
C SI=SINF(FI)
C
C COMPUTE TRUE ANOMALY STEP SIZE
C
C DV=TPI/36.
C I=0
C V=0.
C YA=0.
C YP=0.
C 1 SV=SINF(V)
C CV=COSF(V)
C
C COMPUTE SATELLITE HEIGHT
C
C SP=SI*(SO*CV+CO*SV)
C RE=AF/SQRTF(1.+FE*SP**2)
C REP/(1.+E*CV)

```

NOT REPRODUCIBLE

```

H = R - RE
CALL ATMOS(H,RHO)
F=SQRTF(1.+2.*F*CV+(-E)*RHO)
FA=2.*F*(1.+CV)
FP=2.*F*(1.-CV)
IF(1.EQ.(I/2)*2) GO TO 3
2 FA=2.*FA
FP=2.*FP
3 YA=YA+FA
YP=YP+FP
IF(1.EQ.35) GO TO 4
I=I+1
V=V+DV
GO TO 1
4 YA=YA+DV*SQRTF((1.+E)/(1.-E)**3)/3.
YP=YP+DV*SQRTF((1.-E)/(1.+E)**3)/3.
C
C COMPUTE APOGEE DECAY RATE
C
AHDOT=SDTP*YA*FCOEF.
C
C COMPUTE PERIGEE DECAY RATE
C
PHDOT=SDTP*YP*FCOEF.
C
C COMPUTE SEMI-MAJOR AXIS DECAY RATE
C
ADOT=.5*(AHDOT+PHDOT)
END

```

NOT REPRODUCIBLE

APPENDIX III

SUBROUTINE ELRAT

(Mean Elements Secular Rates Computation - See SECTION II)

Preceding page blank

```

SUBROUTINE ECRAT(AE,E2,FMU,FJ2,B,FM,FN)
C   THE PURPOSE OF THIS ROUTINE IS TO COMPUTE ELEMENT RATES
C   GIVEN MEAN ELEMENTS
C
C   INPUTS ARE
C       AE=EARTH SEMI-MAJOR AXIS(FT)
C       E2=EARTH ECCENTRICITY SQUARED
C       FMU=EARTH GRAVITY CONSTANT(FT**3/SEC**2)
C       FJ2=EARTH GRAVITY SECOND ZONAL HARMONIC COEFFICIENT
C       B=OBJECT BALLISTIC COEFFICIENT (FT**2/LP)
C       FM(1)-(6)=MEAN ELEMENTS AT EPOCH
C           FM(1)=MEAN SEMI-MAJOR AXIS (FT)
C           FM(2)=MEAN ECCENTRICITY
C           FM(3)=MEAN INCLINATION (DEG)
C           FM(4)=MEAN ARGUMENT OF PERIGEE (DEG)
C           FM(5)=MEAN RIGHT ASCENSION OF ASCENDING
C                   NODE (DEG)
C           FM(6)=MEAN MEAN ANOMALY (DEG)
C
C   OUTPUTS ARE
C       FN(1)-(12)=MEAN ELEMENT RATES AT EPOCH
C           FN(1)=MEAN SEMI-MAJOR AXIS (ER=EARTH RADII)
C           FN(2)=ADOT=SEMI-MAJOR AXIS RATE (ER/DAY)
C           FN(3)=ADDOT2 (ER/DAY**2)
C           FN(4)=EDOT=ECCENTRICITY RATE (/DAY)
C           FN(5)=JDOT2 (/DAY**2)
C           FN(6)=JDOT=ARGUMENT OF PERIGEE RATE (DEG/DAY)
C           FN(7)=JDOT2 (DEG/DAY**2)
C           FN(8)=NDOT=RIGHT ASCENSION OF ASCENDING
C                   NODE RATE (DEG/DAY)
C           FN(9)=NDOT2 (DEG/DAY**2)
C           FN(10)=VN=MEAN MOTION (REVS/DAY)
C           FN(11)=VDOT2 (REVS/DAY**2)
C           FN(12)=NDOT06 (REVS/DAY**3)
C
C   DIMENSION FM(6),FN(12)
C   TYPE REAL NV,IR,OB,JDOT,VDOT,NDOT06,NDOT2,NDOT02
C   DATA(DFGRA=57.2957795131),(FK3=360.)
C
C       FK1=240.*DEGRA
C       FK1=FK1*FK1
C       AN=FM(1)/AE
C       EB=FM(2)
C       IB=FM(3)/DEGRA
C       SIB=SINF(IB)
C       CIB=COSEF(IB)
C       OB=FM(4)/DEGRA
C       SOB=SINF(OB)
C       IF(FM(1))51,51,1
1  AB=FM(1)

```

COMPUTE SEMI-MAJOR AXIS

$P = AV * (1. + EB * EB)$

$P2 = P * P$

C

COMPUTE ANOMALISTIC MEAN MOTION

C

$XX = 1.5 * FJ2 * SQRTF(1. - EB * EB) * (1. - 1.5 * SIR * SIB) / P2$

2 $NN = SQRTF(FMU * FK1 * (1. - XX) / (AB * AR * AH))$

C

COMPUTE SECULAR RATES OF ARG. OF PERIGEE AND RT. ASCEN.

C

6 $DDOT = .75 * NN * FJ2 * FK3 * (5. * CIR * CIR - 1.) / P2$

7 $NDDOT = -1.5 * NN * FJ2 * FK5 * CIB / P2$

C

COMPUTE RATES OF SEMI-MAJOR AXIS, ECCENTRICITY AND MEAN MOTION

C

CALL DTPDA(FMU, AE, F2, AR, EB, IB, OB, S, ADOT)

ADOT = ADOT / AE

10 $EDOT = ADOT * (1. - EB) / AN$

$NDDOT2 = -3. * NN * ADOT / (4. * AN)$

COMPUTE ARGUMENT OF PERIGEE AND RIGHT ASCENSION OF ASCENDING NODE

C

ACCELERATION TERMS

$TEMP = NDDOT2 * (1. + 4. * (1. - EB) / (3. * (1. + EB))) / NN$

$DDDDOT2 = DDOT * TEMP$

$NDDOT2 = NDDOT * TEMP$

IF(EB.GE.0.06) GO TO 41

C

COMPUTE SEMI-MAJOR AXIS, ECCENTRICITY AND MEAN

C

MOTION ACCELERATION TERMS

C

$C = NDDOT2 / NN$

ACON = 13.

IF(NN.LE.16.204) ACON = 4.

$D = ACON * C * C * (1. + 16.657 / (3. * (16.667 - NN)))$

11 $ADDDOT2 = AN * (-2. * D + 20. * C * C / 9.)$

12 $NDDDDOT2 = (3. * NN * ADDOT2 + 5. * ADOT * NDDOT2) / (6. * AN)$

$EDDDOT2 = (1. - EB) * ADDDDOT2 / AN$

GO TO 50

41 $ADDDOT2 = 0.$

$NDDDDOT2 = 0.$

$EDDDOT2 = 0.$

50 CONTINUE

C

SET UP OUTPUT ARRAY

C

$FN(1) = AN$

$FN(2) = ADOT$

$FN(3) = ADDOT2$

$FN(4) = EDDOT$

NOT REPRODUCIBLE

FN(5)=E0002
FN(6)=0000
FN(7)=000002
FN(8)=0000
FN(9)=00002
FN(10)=NN
FN(11)=0002
FN(12)=00006
51 CONTINUE
END

NOT REPRODUCIBLE

APPENDIX IV
SUBROUTINE DELTA

(Kozai Short Period Element Variations - See SECTION III.2)

```

SUBROUTINE DELTA (AE,J2,M,I)
C
C THE PURPOSE OF THIS SUBROUTINE IS TO COMPUTE SHORT PERIOD
C ELEMENT EVARIATIONS USING THE KOZAI METHOD.
C
C INPUTS ARE
C   AF=EARTH SEMI-MAJOR AXIS (FT)
C   J2=EARTH GRAVITY SECOND ZONAL HARMONIC COEFFICIENT
C   M(1)=ORBIT MEAN SEMI-MAJOR AXIS (FT)
C   M(2)=MEAN ECCENTRICITY
C   M(3)=MEAN INCLINATION (DEG)
C   M(4)=MEAN ARGUMENT OF PERIGEE (DEG)
C   M(5)=MEAN RIGHT ASCENSION OF ASCENDING NODE (DEG)
C   M(6)=MEAN MEAN ANOMALY (DEG)
C
C OUTPUTS ARE DIFFERENCES (OSCULATING - MEAN) OF ABOVE ELEMENTS
C IN THE SAME UNITS STORED IN D(1) THRU D(6)
C
C   DIMENSION M(6),D(6)
C   TYPE REAL M,J2,JE
C   DATA(PI=3.1415926536),(FK=57.2957795131),(OT=.333333333333)
C   DATA(TT=.666666666667)
C
C   TPI = 2. * PI
C   JE=1.5*J2*AE*AF
C   E=M(2)
C   IF(E)1,2,2
1  E=0
C   M(2)=E
C   GO TO 4
2  IF(E-1.)4,3,3
3  E=.999999999999
C   M(2)=E
4  ESQ=E*E
C   OME2=1.-ESQ
C   SOM=1./OMF2**1.5
C   FM=M(6)/FK
9  IF(ABS(FM)-PI) 10,10,11
C   REDUCE MEAN ANOMALY TO RANGE OF -PI TO +PI
11 FM=FM-TPI*ABS(FM)/FM
C   GO TO 9
C COMPUTE ECCENTRIC ANOMALY
10 EP=FM
C   DO 14 J=1,10
C   EA=EP-(EP-M(2)*SINF(EP)-FM)/(1.-M(2)*COSF(EP))
C   IF(ABS(EA-EP).LT.1.E-10) GO TO 20
14 EP=EA
C COMPUTE TRUE ANOMALY
20 V=2.*ATAN2(SQRT((1.+E)/(1.-E))*SINF(EA*.5),COSF(EA*.5))

```



```

      IF(FM) 30,31,31
30  FM=FM+TPI
31  IF(V) 32,33,33
32  V=V+TPI
33  IF(V-TPI) 34,35,35
35  V=V-TPI
34  AB=M(1)
      FI=M(3)/FK
      FO=M(4)/FK
      FN=M(5)/FK
      COMPUTE RADIUS AND SEMI-LATUS RECTUM
      R=AB*(1.-M(2)*COSF(EA))
      P=AB*OME2
      P2=P*P
      AOR3=(AB/R)**3
      COMPUTE VARIOUS FUNCTIONS OF SINE AND COSINE OF
C   INCLINATION, TRUE ANOMALY, AND ARGUMENT OF PERIGEE
      SI2=(SINF(FI))**2
      SFI=1.-1.5*SI2
      SV=SINF(V)
      CV=COSF(V)
      SO=SINF(FO)
      CO=COSF(FO)
      SV0=SV*CO+CV*SO
      CV0=CV*CO-SV*SO
      S2V=2.*SV*CV
      C2V=2.*CV*CV-1.
      S3V=SV*(3.-4.*SV*SV)
      C3V=CV*(4.*CV*CV-3.)
      S4V=SV*C3V+CV*S3V
      C4V=CV*C3V-SV*S3V
      S5V=S2V*C3V+C2V*S3V
      C5V=C2V*C3V-S2V*S3V
      S20=2.*SO*CO
      C20=2.*CO*CO-1.
      S2V0=2.*SV0*CV0
      C2V0=2.*CV0*CV0-1.
      SV20=SV*C20+CV*S20
      CV20=CV*C20-SV*S20
      S3V20=S3V*C20+C3V*S20
      C3V20=C3V*C20-S3V*S20
      SVM20=SV*C20-CV*S20
      S4V20=S4V*C20+C4V*S20
      S5V20=S5V*C20+C5V*S20
      COMPUTE KOTA SHORT PERIOD VARIATIONS
      D(1)=(JE/AB)*(SFI*TT*(AOR3-SOM)+AOR3*SI2*C2V0)
      DE1=JE*OME2/(AB*AB*E)*(D1*SFI*(AOR3-SOM)+.5*AOR3*SI2*C2V0)
      DE2=JE*SI2/(2.*AB*E*P)*(C2V0+E*CV20+OT*E*C3V20)
      D(2)=DE1-DE2

```

```

D(3)=JE*SINF(2.*F1)/(4.*P2)*(C2V0+E*CV20+OT*F*C3V20)*FK
D01=(2.-2.5*S12)*(V-FM+E*SV)+SF1*(1.-.25*ESQ)*SV/F+
1 .5*S2V+F*S3V/12.)
D02=-SV20/F*(.25*S12+ESQ*(.5-.9375*S12))+.0625*E*S12*SVM20
D03=-.5*(1.-2.5*S12)*S2V0+S3V20/E*(7.*S12/12.-ESQ+
1 (1.-19.*S12/8.)/6.)
D04=.375*S12+S4V20+.0625*E*S12*S5V20-.375*S12*S20
D(4)=JE/P2*(D01+D02+D03+D04)*FK
D(5)=-JE*COSF(F1)/P2*(V-FM+E*SV-.5*S2V0-.5*E*SV20-
1 E*S3V20/6.)*FK
DM1=-SF1*((1.-.25*ESQ)*SV+.5*E*S2V+ESQ*S3V/12.)
DM2=S12*(.25*SV20*(1.+1.25*ESQ)-.0625*ESQ*SVM20-
1 7.*S3V20/12.+
2 (1.-ESQ/28.))- .375*E*S4V20-.0625*ESQ*S5V20+.375*F*S20)
D(6)=JE/(E*P2)*SORTF(DME2)*(DM1+DM2)*FK
END

```

NOT REPRODUCIBLE

APPENDIX V

SUBROUTINE DELXYZ

**(Frazer Long and Short Period Element
Variations - See SECTION III.3)**

SUBROUTINE DELXYZ(A,FMU,FJ2,FJ3,XYZ,DES)

C THIS SUBROUTINE ACCEPTS MEAN CARTESIAN ELEMENTS AND
C COMPUTES THE DIFFERENCES BETWEEN MEAN AND OSCULATING
C CARTESIAN ELEMENTS. REFERENCE IS FRAZER, SEPT. 1966.

C INPUTS ARE

C AE=EARTH SEMI-MAJOR AXIS (FT)
C FMU=EARTH GRAVITY CONSTANT (FT**3/SEC**2)
C FJ2=EARTH GRAVITY SECOND ZONAL HARMONIC COEFFICIENT
C FJ3=EARTH GRAVITY THIRD ZONAL HARMONIC COEFFICIENT
C XYZ(1),XYZ(2),XYZ(3)=MEAN POSITION COMPONENTS IN AN
C EARTH-CENTERED, EQUATORIAL, INERTIAL, RIGHT-HANDED,
C CARTESIAN SYSTEM, WITH (1) TOWARD THE VERNAL
C EQUINOX AND (3) THRU THE NORTH POLE (FT)
C XYZ(4),XYZ(5),XYZ(6)=VELOCITY COMPONENTS IN
C ABOVE SYSTEM (FT/SEC)

C OUTPUTS ARE

C DES(1) - (6)=PERIODIC VARIATIONS IN CARTESIAN ELEMENTS
C (OSCULATING-MEAN) (FT) AND (FT/SEC)

DIMENSION XYZ(6),DES(6)

IF(FJ2.EQ.0.) GO TO 10

X=XYZ(1)

Y=XYZ(2)

Z=XYZ(3)

XD=XYZ(4)

YD=XYZ(5)

ZD=XYZ(6)

SMU=SQRTF(FMU)

COMPUTE RADIIIS

RAD=SQRTF(X*X+Y*Y+Z*Z)

COMPUTE INVERSE OF SEMI-MAJOR AXIS

V2=XD*XD+YD*YD+ZD*ZD

AINV=(2.*FMU-RAD*V2)/(FMJ*RAD)

IF(AINV.LE.0.) GO TO 10

HX=Y*ZD-YD*Z

HY=-X*ZD+XD*Z

HZ=X*YD-XD*Y

HXY2=HX*HX+HY*HY

H2=HXY2+HZ*HZ

H=SQRTF(H2)

COMPUTE INCLINATION

SINI=SQRTF(HXY2)/H

IF(SINI.LT.0.0017) GO TO 10

COSI=H2/H

HSINI=H*SINI

COMPUTE RT. ASC. OF ASC. NODE

SINN=HX/HSINI

NOT REPRODUCIBLE

NOT REPRODUCIBLE

COSN=-HY/H*INT
 COMPUTE ARG. OF LATITUDE
 SINU=/(RAD*SINI)
 COSU=(X*HY+Y*HX)/(RAD*HSINI)
 SIN2U=2.*SINU*COSU
 COS2U=1.-2.*SINU*SINU
 RDOTV=X*XD+Y*YD+Z*ZD
 COMPUTE RADIUS RATE
 RADD=RDOTV/RAD
 ESINV=RADD*H/FMU
 COMPUTE SEMI-LATUS RECTUM
 P=H2/FMU
 SQP=SQRT(P)
 ECOSV=(P/RAD)-1.
 OPECV=1.*ECOSV
 COMPUTE RADIUS TIMES TRUE ANOMALY RATE
 RVD=SMU*OPECV/SQP
 COMPUTE ECCENTRICITY SQUARED
 E2=ESINV*ESINV+ECOSV*ECOSV
 IF(E2.GE.1.) GO TO 10
 ETA=SQRT(1.-E2)
 COMPUTE TRUE MINUS MEAN ANOMALY
 SVME=(ESINV/OPECV)*((ETA+OPECV)/(1.+ETA))
 IF(ABS(SVME).GT.1.) GO TO 10
 VMM=ASIN(SVME)+ETA*ESINV/OPECV
 COMPUTE SHORT PERIOD PERTURBATIONS IN SPECIAL ELEMENTS
 SI2=SINI*SINI
 CI2=COSI*COSI
 SCI2=1.-3.*CI2
 PEE=P/AE
 ALPHA=.25*FJ2/(PEE*PEE)
 ALFA1=ALPHA*SMU/SQP
 FS2UMV=ECOSV*SIN2U=-SINV*COS2U
 EC2UMV=ECOSV*COS2U=-SINV*SIN2U
 ES2UPV=ECOSV*SIN2U=-SINV*COS2U
 EC2UPV=ECOSV*COS2U=-SINV*SIN2U
 DESR=ALPHA*P*(SI2*CJS2U+SCI2*(1.-1.*ETA/OPECV+ECOSV/
 1 (1.+ETA)))
 TEMP=OPECV*OPECV
 DESRD=-ALFA1*(2.*SI2*TEMP*SIN2U+SCI2*ESINV*
 1 (-.5*ETA+TEMP/(1.+ETA)))
 DESRVD=SI2*(2.*COS2U+2.*EC2UMV+ECOSV*COS2U)
 DESRVD=DESRVD-SCI2*(1.5+ECOSV*((2.+ETA)/(1.+ETA))+
 1 .5*(E2-2.*ESINV*ESINV)/(1.+ETA))
 DESRVD=RVD*ALPHA*DESRVD
 DESI=ALPHA*SINI*COSI*(3.*(COS2U+EC2UMV)+EC2UPV)
 DESN=-ALPHA*COSI*(6.*(VMM+ESINV)-3.*(SIN2U+ES2UMV)-ES2UPV)
 DESU=6.*(1.-5.*CI2)*VMM+4.*(1.-6.*CI2+SCI2/(1.+ETA))*ESINV
 DESU=DESU+SCI2*2.*ESINV*ECOSV/(1.+ETA)+2.*(5.*CI2-2.)*
 1 ES2UMV

NOT REPRODUCIBLE

```

DESU=DESU*(7.*CT2-1.)*SIN2U+7.*CT2*E320PV
DESU=.5*ALPHA*DESU
COMPUTE SHORT PERIOD PERTURBATIONS IN CARTESIAN ELEMENTS
XU=COSU*COSN-SINU*SINN*COSI
YU=COSU*SINN+SINU*COSN*COSI
ZU=SINU*SINI
XV=-SINU*COSN-COSU*SINN*COSI
YV=-SINU*SINN+COSU*COSN*COSI
ZV=COSU*SINI
XW=SINN*SINI
YW=-COSN*SINI
ZW=COSI
TEMP=DESU+COSI*DESN
TEM=SINU*DESI-COSU*SINI*DESN
DESX=DESR*XU+RAJ*(TEMP*XV+TEM*XW)
DESY=DESR*YU+RAJ*(TEMP*YV+TEM*YW)
DESZ=DESR*ZU+RAJ*(TEMP*ZV+TEM*ZW)
TC=DESRD-RVD*TEMP
TD=DESRVD+RADN*TEMP
TE=RADN*TEM+RVN*(COSU*DESI+SINU*SINI*DESN)
DESXD=TC*XU+TD*XV+TE*XW
DESYD=TC*YU+TD*YV+TE*YW
DESZD=TC*ZU+TD*ZV+TE*ZW
COMPUTE LONG PERIOD PERTURBATIONS IN CARTESIAN ELEMENTS
ALFA2=.5*FJ3/(FJ2*P-E)
ESU=SINU*ECOSV-COSU*ESINV
TA=SINI*OPECV*(ALFA2*SINU)
TB=SINI*(ALFA2*(1.+JPECV)*COSU)
TC=COSI*(ALFA2*ECOSV)
TD=-SINI*OPECV*(ALFA2*COSU)
TE=-SINI*(ALFA2*(SINU+ESU))
TF=-COSI*(ALFA2*ESINV)
DELX=RAD*(TA*XU+TB*XV+TC*XW)
DELY=RAD*(TA*YU+TB*YV+TC*YW)
DELZ=RAD*(TA*ZU+TB*ZV+TC*ZW)
TEM=SMU/SQP
DELXD=TEM*(TD*XU+TE*XV+TF*XW)
DELYD=TEM*(TD*YU+TE*YV+TF*YW)
DELZD=TEM*(TD*ZU+TE*ZV+TF*ZW)
GO TO 20
10 CONTINUE
DESX=DESY=DESZ=DESXD=DESYD=DESZD=0.
DELX=DELY=DELZ=DELXD=DELYD=DELZD=0.
20 CONTINUE
DES(1)=DESX+DELX
DES(2)=DESY+DELY
DES(3)=DESZ+DELZ
DES(4)=DESXD+DELXD
DES(5)=DESYD+DELYD
DES(6)=DESZD+DELZD
END

```

APPENDIX VI

SUBROUTINE OSMCE

(Iteration Control for Computing Mean From
Osculating Elements - See SECTION III.4)

SUBROUTINE OSRCE(AE,FM1,FJ2,FJ3,XYZ,XYZ4)

```

C
C THE PURPOSE OF THIS SUBROUTINE IS TO COMPUTE MEAN FROM
C OSCULATING CARTESIAN ELEMENTS ITERATIVELY USING DELXYZ
C
C INPUTS ARE
C AE=EARTH SEMI-MAJOR AXIS (FT)
C FM1=EARTH GRAVITY CONSTANT (FT**3/SEC**2)
C FJ2=EARTH GRAVITY SECOND ZONAL HARMONIC COEFFICIENT
C FJ3=EARTH GRAVITY THIRD ZONAL HARMONIC COEFFICIENT
C XYZ(1),XYZ(2),XYZ(3)=OSCULATING POSITION COMPONENTS
C IN AN EARTH-CENTERED, EQUATORIAL, INERTIAL,
C RIGHT-HANDED CARTESIAN SYSTEM, WITH (1) TOWARD
C THE VERNAL EQUINOX AND (3) TOWARD THE NORTH POLE (FT)
C XYZ(4),XYZ(5),XYZ(6)=VELOCITY COMPONENTS IN
C ABOVE SYSTEM (FT/SEC)
C
C OUTPUTS ARE
C XYZM(1)-(6)=MEAN POSITION AND VELOCITY COMPONENTS IN
C SYSTEM SIMILAR TO ABOVE (FT) AND (FT/SEC)
C
C DIMENSION XYZ(6),DES(6),XYZM(6),DXYZ(6)
C ESTABLISH INITIAL ESTIMATE OF MEAN ELEMENTS
DO 1 J=1,6
XYZM(J)=XYZ(J)
1 CONTINUE
I=0
2 CONTINUE
I=I+1
CALL DELXYZ(AE,FM1,-J2,FJ3,XYZM,DES)
IF(I.NE.1) GO TO 4
C IMPROVE ESTIMATE OF MEAN ELEMENTS
DO 3 J=1,6
XYZM(J)=XYZ(J)-DES(J)
3 CONTINUE
GO TO 2
4 CONTINUE
C IMPROVE ESTIMATE OF MEAN ELEMENTS
DO 5 J=1,6
DXYZ(J)=XYZ(J)-XYZM(J)-DES(J)
XYZ4(J)=XYZM(J)+DXYZ(J)
5 CONTINUE
C TEST FOR CONVERGENCE
IF(I.EQ.10) GO TO 8
DO 6 J=1,3
IF(ABS(DXYZ(J)).GT.1.) GO TO 2
6 CONTINUE
DO 7 J=4,6
IF(ABS(DXYZ(J)).GT.0.001) GO TO 2

```


7 CONTINUE
6 CONTINUE
END

APPENDIX VII
SUBROUTINE UPDAT

(Analytical Trajectory Generator - See SECTION IV.2)

Preceding page blank

```

SUBROUTINE UPDAT(TN,XM,XN,DAY,FDAY,A,E,FI,FO,FN,FM)
C   THE PURPOSE OF THIS SUBROUTINE IS TO PERFORM TRAJECTORY
C   GENERATION USING MEAN ELEMENT SECULAR VARIATIONS AND A
C   MACLAURIN'S SERIES EXPANSION.
C   INPUTS ARE
C   TN(1)=INTEGER PORTION OF EPOCH (DAYS)
C   TN(2)=FRACTIONAL PORTION OF EPOCH (DAYS)
C   XM(1)-(6) AND XN(1)-(12) ARE THE MEAN ELEMENTS AND
C   THEIR RATES AT EPOCH.
C       XM(1)=MEAN SEMI-MAJOR AXIS (ET)
C       XM(2)=MEAN ECCENTRICITY
C       XM(3)=MEAN INCLINATION (DEG)
C       XM(4)=MEAN ARGUMENT OF PERIGEE (DEG)
C       XM(5)=MEAN RIGHT ASCENSION OF
C           ASCENDING NODE (DEG)
C       XM(6)=MEAN MEAN ANOMALY (DEG)
C       XN(1)=MEAN SEMI-MAJOR AXIS (ET=EARTH RADIUS)
C       XN(2)=ADOT=SEMI-MAJOR AXIS RATE (ET/DAY)
C       XN(3)=ADOT2 (ET/DAY**2)
C       XN(4)=EDOT=ECCENTRICITY RATE (/DAY)
C       XN(5)=EDOT2 (/DAY**2)
C       XN(6)=JDOT=ARGUMENT OF PERIGEE RATE (DEG/DAY)
C       XN(7)=JDOT2 (DEG/DAY**2)
C       XN(8)=NDOT=RIGHT ASCENSION OF ASCENDING
C           NODE RATE (DEG/DAY)
C       XN(9)=NDOT2 (DEG/DAY**2)
C       XN(10)=NN=MEAN MOTION (REVS/DAY)
C       XN(11)=NDOT2 (REVS/DAY**2)
C       XN(12)=NDOT3 (REVS/DAY**3)
C   DAY=INTEGER PORTION OF TIME OF UPDATED ELEMENTS (DAYS)
C   FDAY=FRACTIONAL PORTION OF TIME OF
C       UPDATED ELEMENTS (DAYS)
C   OUTPUTS ARE
C       A=UPDATED MEAN SEMI-MAJOR AXIS (ET)
C       E=UPDATED MEAN ECCENTRICITY
C       FI=UPDATED MEAN INCLINATION (DEG)
C       FO=UPDATED MEAN ARGUMENT OF PERIGEE (DEG)
C       FN=UPDATED MEAN RIGHT ASCENSION OF ASCENDING NODE (DEG)
C       FM=UPDATED MEAN MEAN ANOMALY (DEG)
C   DIMENSION TN(2),XM(6),XN(12)
C   DELT=(DAY-TN(1))+(FDAY-TN(2))
C   DELT2=DELT*DELT
C   A=XN(1)+DELT*XN(2)+DELT2*XN(3)
C   E=1.-(XN(1)*(1.-XM(2)))/A
C   FI=XM(3)

```

NOT REPRODUCIBLE

```

      FD=XM(4)*XN(6)*DELT+XN(7)*DELT2
      FN=XM(5)*XN(8)*DELT+XN(9)*DELT2
      FM=XM(6)*360.*(XN(10)*DELT+XN(11)*DELT2+XN(12)*DELT*DELT2)
C      REDUCE MEAN ANOMALY TO RANGE OF 0 TO 360
      FM=MODF(FM,360.)
      IF(FM.LT.0.) FM=FM+360.
      END

```

NOT REPRODUCIBLE

REFERENCES

1. Y. Kozai, "The Motion of a Close Earth Satellite," Astronomical Journal, November 1959, Vol. 64, No. 1274.
2. C. G. Hilton, "The SPADATS Mathematical Model", Aeronutronic ESD-TDR-63-427, 5 August 1963.
3. C. G. Hilton and J. R. Kuhlman, "Mathematical Models for the Space Defense Center," Aeronutronic U-3871, 30 November 1966.
4. A. R. McNair and E. P. Boykin, "Earth Orbital Lifetime Prediction Model and Program," NASA TM X-53385, N66 28021, 1 February 1966.
5. Purcell and Cowan, "Relating Geodetic Latitude and Altitude to Geocentric Latitude and Radius Vector," ARS Journal, Vol. 31, No. 7, July 1961.
6. R. W. Wolverton, Flight Performance Handbook for Orbital Operations, Space Technology Laboratories, September 1961.
7. J. B. Frazer, "On the Motion of an Artificial Earth Satellite," Mitre Corporation, ESD-TR-66-293, September 1966.
8. R. M. L. Baker, Astrodynamics: Applications and Advanced Topics (Appendix C), Academic Press, 1967.
9. H. G. Walter, "Conversion of Osculating Orbital Elements into Mean Elements," Astronomical Journal, Vol. 72, No. 8, October 1967.
10. J. A. Ward, Jr., "Automatic Multi-Satellite Ephemeris Maintenance", Air Force Eastern Test Range, ETR-TR-71-1, August 1971.